



**POTENT INHIBITORS DESIGNED FOR METHIONINE
AMINOPEPTIDASE II USING PHARMOCOPHORE
MODELING**

SAFANAH A. AL-BAYATI

MASTER'S THESIS

Submitted to the Graduate School of Science and Engineering of
Kadir Has University in partial fulfillment of the requirements for the degree of
Master of Science in In the Program of Computational Biology and Bioinformatics

İSTANBUL, JANUARY, 2019

DECLARATION OF RESEARCH ETHICS /
METHODS OF DISSEMINATION

I, SAFANAH A. AL-BAYATI, hereby declare that;

- this master's thesis is my own original work and that due references have been appropriately provided on all supporting literature and resources;

In addition, I understand that any false claim in respect of this work will result in disciplinary action in accordance with University regulations.

Furthermore, both printed and electronic copies of my work will be kept in Kadir Has Information Center under the following condition as indicated below:

- The full content of my thesis will be accessible from everywhere by all means.
thesis will be automatically accessible from everywhere by all means.

SAFANAH A. AL-BAYATI

4.1.2019

KADİR HAS UNIVERSITY
GRADUATE SCHOOL OF SCIENCE AND ENGINEERING

ACCEPTANCE AND APPROVAL

This work entitled POTENT INHIBITORS DESIGNED FOR METHIONINE AMINOPEPTIDASE II USING PHARMOCOPHORE MODELING prepared by SAFANAH A. AL-BAYATI has been judged to be successful at the defense exam on 4.1.2019 and accepted by our jury as

APPROVED BY:

Prof. Dr. Kemal Yelekçi (Advisor)
Kadir Has University

Asst.Dr. Hatice Bahar ŞAHİN
Kadir Has University

Asst.Dr.Vildan ENİSOĞLU ATALAY
Uskudar University

I certify that the above signatures belong to the faculty members named above.

.....
Asst. Prof. Dr.Demet Akten Akdoğan
Dean of Graduate School of Science and Engineering

DATE OF APPROVAL: 4.1.2019

TABLE OF CONTENTS

ABSTRACT	i
ÖZET	ii
ACKNOWLEDGEMENTS	iii
DEDICATION	iv
LIST OF TABLES	v
LIST OF FIGURES	vi
LIST OF SYMBOLS/ABBREVIATIONS	viii
1. Objective	1
2. INTRODUCTION	2
2.1 Cancer	2
2.1.1 Non-small-cell lung cancer (NSCLC)	3
2.2 Rheumatoid arthritis (RA)	4
2.3 Obesity	5
2.4 Angiogenesis	7
2.5 Methionine (Met)	8
2.6 Methionine aminopeptidase II	9
2.7 Computer aid drug design	10
2.7.1 Pharmacophore	11
2.7.2 Virtual screening	11
2.7.3 ADMET Prediction Test	12
3. MATERIALS AND METHOD	13
3.1 Database Preparation	15
3.2 Ligand-Based Approach	16
3.2.1 Protein Preparation	16
3.2.2 Known Inhibitor, Molecular Docking Validation	16
3.2.3 Data sets	20
3.2.4 Pharmacophore Generation	22
3.3 Structure-Based Approaches	24

3.3.1	Further Filtration	25
3.3.2	Protein Preparation	25
3.3.3	Pharmacophore Generation	26
3.4	Pharmacophore validation	33
3.5	Virtual Screening	37
3.6	PyRx	37
3.7	AutoDock	38
4.	RESULTS AND DISCUSSION	39
	REFERENCES	50



POTENT INHIBITORS DESIGNED FOR METHIONINE AMINOPEPTIDASE
II USING PHARMOCOPHORE MODELING

ABSTRACT

Methionine Aminopeptidase (Metap2) is a metalloenzyme that is responsible of removing of the N-terminal of newly synthesized protein. The inhibition of the enzyme was found to be crucial in diminishing tumor's nourishment, growth, and metastasis. It is directly related to incurable diseases such as Cancer, Rheumatoid Arthritis, etc. Over the year, different compounds were developed to inhibit that enzyme. Fumagillin, a natural irreversible inhibitor of MetAP2 and its derivatives, has been showing great potential therapy, however, their toxicity and poor pharmacokinetic characteristics have forbidden them from passing clinical trial and FDA approval. In this research, an in-silico approach was conducted to obtain a compound that is capable of inhibiting the enzyme with non-toxic properties. Two different approaches were conducted using a pharmacophore modeling; Ligand-Based, and Structure-Based. The Zinc15 and National Institute of Cancer Data (NCI) Databases was screened to obtain diversity of pre-synthesized compound. Followed by Molecular Docking filtration process using PyRx, and Autodock4. Followed by Discovery Studios protocol called ADMET prediction to signify the ability of these compound to pass the blood barriers and demonstrate better pharmacokinetics properties than the Fumagillian. These compounds will serve, as Great Drug Candidate for the biological test in our continuous war against cancer and others Incurable disease.

Keywords: Metap2, Pharmacophore modeling, Drug design, Autodock4

TEZİN TÜRKÇE ADI

ÖZET

Metaloenzimlerden Metiyonin Aminopeptidazlar (MetAP2), yeni sentezlenmiş polipeptitlerin başından metionin amino asidini kesmekle sorumludur. MetAP2'nin seçimli olarak engellenmesi damar oluşumunu baskıladığı, katı tümörlerde tümör boyunu ve metastazı sınırladığı gösterilmiştir. Romatizma, kanser v.b. gibi tedavisi zor hastalıklarla direkt ilgili olduğu bulunmuştur. Araştırmacılar uzun süredir bu enzimi inhibe eden ilaçlar üzerine çalışmaktadır. Fumagillin MetAP2'nin doğal geri dönüşümsüz inhibitörüdür. Fumagillin ve yarı sentetik analogları potansiyel ilaç olarak umut vaat etmelerine karşı farmakokinetik ve nörotoksik özelliklerinden dolayı FDA'dan klinik deneyler için izin alamamıştır. Bu çalışmada, Zinc15 ve Ulusal Kanser Enstitüsü (NCI) veri bankalarından MatAP2'nin potansiyel ve toksik olmayan inhibitörleri in silico tarama, ligand ve yapı bazlı farmakofor modelleme yöntemleri ile elde edilmiştir. PyRx ve Doklama işlemleri ile uygulanarak aralarından daha isabetli ilaç adayları seçilmiştir.

Discovery Studio (2016)'nın ADMET protokolü adayların farmakokinetik özelliklerini tespiti için kullanılmıştır. Bulunan bu adaylar MetAP2 enzimine potansiyel inhibitör olabilecekleri ve farmakokinetik özelliklerinin Fumagillin'dan daha iyi oldukları bulunmuştur. Bulunan bu moleküller biyolojik testler için ve tedavisi zor kanser ve bu gibi hastalıklara karşı çok iyi potansiyel ilaç adayları olacağı görüşüne varılmıştır.

Anahtar Sözcükler:

ACKNOWLEDGEMENTS

First, I would like to praise Allah for granting me this wonderful opportunity. I would, also, like to acknowledge and thank my supervisor, Dr. Kemal Yelekci, for his guidance and superb mentorship throughout my studies and thank Dr. ABDULLAHI IBRAHIM UBA for his motivations speak and his advice that keeps me working.

I also want to express my gratitude to my parents and siblings, for supporting me through this challenging journey.

Finally, I extend a heartfelt to my aunt Fatima, the faculty members at the computational Biology and Bioinformatics department, my friends, and colleagues in the laboratory.

Dedication

I dedicate this work to those who are always very close to my heart, my father Zaid Al-Bayati and my mother Nawal Al-Hamdany.



LIST OF TABLES

Table 3.1	3.1 The known ligand used for validation of the macromolecule .	18
Table 3.2	The Data set that was used to obtain the common pharmacophore feature	21
Table 3.3	The Training set that was used to validate the pharmacophore hypothesis-1	34
Table 3.4	The Training set that was used to validate the pharmacophore hypothesis-2	35
Table 3.5	The pharmacophore validation result for both Ligand-Based approaches, and Structure-Based approaches.	36
Table 4.1	Ligand-Based approaches the resulting compounds and their properties.	40
Table 4.2	Structure-Based approaches the resulting compounds and their properties.	41
Table 4.3	Structure-Based Cross-Docking between the different PDB Macromolecules.	41

LIST OF FIGURES

Figure 2.1	The two suggested mechanism of action of MetAP2 where (A) Tetrahedral intermediate alleviated by Glu204 and metal center and (B) Tetrahedral intermediate alleviated His178 and metal center (Lowther et al., 1999)	10
Figure 2.2	Pathway of the Pharmacophore Model (Andricopulo, Salum and Abraham, 2009)	12
Figure 3.1	The procedure and the criteria that were followed while choosing the best inhibitor	13
Figure 3.2	2D scheme showing diverse interactions such as Vander Waals, pi-sigma, Carbon Hydrogen bond, etc. between the receptor and Fumagillin	17
Figure 3.3	2D scheme showing diverse interactions such as Vander Waals, pi-sigma, pi-Sulfur, pi-Alkyl etc. Between the receptor and Compound 29	19
Figure 3.4	2D scheme showing diverse interactions such as Vander Waals, pi-sigma, Carbon Hydrogen bond, etc. Between the receptor and 5C	19
Figure 3.5	The compound that form the ligand based approach	22
Figure 3.6	The Hypothesis that was generated using the data set obtained from the literature, the blue ball represented the hydrophobic feature while the green is the hydrogen bond acceptor	23
Figure 3.7	The two compounds 5n and A-310840 from the Data set aligning together and Mapping the pharmacophore hypothesis where the green represents hydrogen bond acceptor and the blue is the hydrophobic feature	23
Figure 3.8	The Inhibitors Compound 8 and AGM-1470, from the Data, set aligning together and Mapping the pharmacophore hypothesis where the green represents hydrogen bond acceptor and the blue is the Hydrophobic feature	24

Figure 3.9	The phylogenetic tree of all input PDB structure	25
Figure 3.10	pharmacophore hypothesis of 5D6E complex	27
Figure 3.11	Best pharmacophore model of 1BOA complex	28
Figure 3.12	1BOA: MetAP2 in complex with Fumagillin	28
Figure 3.13	best pharmacophore model of 1QZY complex	29
Figure 3.14	1QZY:MetAP2 in complex with LAF153 interacting in 2D	30
Figure 3.15	best pharmacophore model of 5D6F complex	31
Figure 3.16	Best pharmacophore model of 5D6F complex	32
Figure 4.1	2D scheme Structure of the Inhibitor from the Ligand-Based approach's	42
Figure 4.2	2D scheme Structure of the Inhibitor from the Structure-Based approach's	43
Figure 4.3	3D Interaction diagram between the amino acid residues and the binding pocket of 1BOA and ZINC000015831093	44
Figure 4.4	3D Interaction diagram between the amino acid residues and the binding pocket of 5D6E and ZINC000015831093	44
Figure 4.5	3D Interaction diagram between the amino acid residues and the binding pocket of 5D6F and ZINC000015831093	45
Figure 4.6	3D Interaction diagram between the amino acid residues and the binding pocket of 1BOA and ZINC000015870630	45
Figure 4.7	3D Interaction diagram between the amino acid residues and the binding pocket of 5D6E and ZINC000015870630	46
Figure 4.8	3D Interaction diagram between the amino acid residues and the binding pocket of 5D6F and ZINC000015870630	46
Figure 4.9	3D Interaction diagram between the amino acid residues and the binding pocket of 5cls and ZINC000012999580	47
Figure 4.10	3D Interaction diagram between the amino acid residues and the binding pocket of 5cls and ZINC000012222765	47
Figure 4.11	The calculated ADMET properties for the Ligand-Based inhibitors	48
Figure 4.12	The calculated ADMET properties for the Structure-Based in- hibitors	48

LIST OF SYMBOLS/ABBREVIATIONS

Metap2	Methionine aminopeptidase 2 is an enzyme found in humans.
NSCLC	Non-small-cell lung cancer.
NCI	National Institute of Cancer Database.
IC50	is the concentration of medication at which 50 percent of your enzyme is inhibited.
ADME	absorption, distribution, metabolism, and excretion
PyRx	is a Virtual Screening tool used to dock compounds of interest against Macromolecule.
IUPAC	International Union of Pure and Applied Chemistry

1. Objective

Methionine Aminopeptidase (MetAPs) is a "metalloenzyme" found in humans in two forms, MetAP1 and MetAP2. The main role of Methionine amino peptide is removing N-terminal initiator methionine from the newly synthesized protein. If the methionine is not removed by MetAPs, it will be non-functional and cleaved by cell mechanism. Recent research has suggested the catalytic actions of MetAP2 on angiogenesis; inhibition of MetAP2 limits the formation of newly formed blood vessels, decreasing tumor nourishment, thus limiting cancer growth. Fumagillin and its derivatives are potent natural inhibitors of MetAP2, demonstrating high ligand selectivity by the enzyme. Fumagillin has limited human application, the U.S. Food and Drug Administration found the biomolecule inadmissible in clinical trials due to its toxicity. Nevertheless, in this research, these compounds are used as a template to screen for potential analogs that are similar in selectivity and affinity toward MetAP2 in an approach called Ligand-based pharmacophore modeling, which extracts common features between known inhibitors and screen for potential ligand analogs. The second approach that is used in this research is structure-based pharmacophore modeling which implements the receptor-ligand binding pocket to create a feature that's later use in screening. Both Zinc15 and National Institute of Cancer (NCI) databases will be obtained for the screening, where only commercially available, a drug-like compound will be a screen. The main principle that was addressed in this research is to produce easily synthesized, highly selective, non-toxic compounds that will be a good candidate for the further biological study.

2. INTRODUCTION

2.1 Cancer

Cells are the basic unit of a living organism, the building block of the body, every day they grow old and die and new cells need to be constructed, as a consequence errors may arise during this process causing a disease. Cancer is an abnormal cell growth that arises from misinterpretation of genes (Alberts et al., 2002). Cancer may arise from different causes, every year the percentage of people who pass away from cancer because of smoking cigarettes is 22. Over 10 percent of deaths come from overweight and alcoholism. Around 5 to 10 percent of cancer can be genetically inherited from the mother or father who have abnormalities in their genes. Living a healthy lifestyle, practicing sport, maintaining a weight limit, avoiding getting too much sun exposure, these simple life choices can reduce the risk of developing cancer disease (Jayasekara et al., 2016), (Anand et al., 2008), (Kushi et al., 2006). Normal cells require signals to carry the information required to begin the growth of the cell or to eliminate it. These signals are usually resembled in a small ligand. The ligand takes the form of growth factor or inhibitors or other forms. The signals communicate through the cell using protein receptors which take place upon the surface of the cell where ligands are bound. Each ligand binds in the binding pocket of the specific receptor to trigger a certain effect. Some common characteristics found in most cancers are uncontrolled cell proliferation, loss of apoptosis, tissue invasion and metastasis, and angiogenesis (Martin et al., 2013). These characteristics are considered a potential therapeutic pathway in which cancer can be stopped and treated. By targeting ligand, receptor, intercellular second messenger, and nuclear transcription factor, responsible for tumor growth, an anti-cancer agent can be designed (Alberts et al., 2002).

2.1.1 Non-small-cell lung cancer (NSCLC)

Lung Cancer is a type of cancer that attack the lungs; the chances of survival perish/ fade away as the disease continues evolving. World health organization show that lungs cancer is the most common type of cancer with 2 million cases around the world. Also it's the first in the list of the most common cause of death with over one million per year. It is responsible for 20 % of all types of cancer deaths around the world. Currently, the most effective approach used now days is the definitive surgical(Kauczor et al., 2015). Lung Cancer is categorized into two types small-cell lung cancer (SCLC) and the Non-small-cell lung cancer (NSCLC),According to a study was conducted with human NSCLC it manifests the crucial role of MetAP2 in treating cancer. MetAP2 is highly expressed in NSCLC tissues. The correlating metastasis gene product S100A4 cooperates with MetAP2 by its nature as angiogenesis against it has led to believe that it helps the cancer cell migration and growth by providing resources to the malignant cell to survive. In the Absent of MetAP2 expression, the chances of the patient to pull through is (85 %) while in the present of Metap2 expression it rises to (55 %). Fumagillin is a natural product and antiangiogenic agent that is used to prevent the growth of NSCLC cell line, hence, increases the apoptosis and decreases the growth of squamous cell carcinoma(SCC) (Shimizu et al., 2016).

2.2 Rheumatoid arthritis (RA)

Rheumatoid arthritis (RA) is a chronic disease that occurs in joints, hands, and feet. It is an autoimmune disease where the immune system instead of defending the organism against external threats starts to attack itself. The disease affects the lifestyle of its patient, causing them to reduce their activity; it is accompanied by joint tenderness, aches, tumescence, and limiting the joint activity. RA is the most common kind of autoimmune condition in the world with around eight hundred thousand individual cases every year only in America. Drugs used in this disease are associated with several side effects and also has a limited effect on the treatment process (Bainbridge et al., 2007).

The angiogenesis process is correlating exponentially with the increasing level of the inflammatory rheumatoid arthritis disease. Angiogenesis, the process of formation of new blood vessels, is in fact accelerating the swelling of the joints. Hence, abnormal migration of a different kind of cell into the joint requires oxygen and nutrition by which it increases the tumescence of the joints. MetAP-2 is an enzyme that was found to be involved in the angiogenesis process by the increasing proliferation of the endothelial cell.

Recently the PPI-2458, a potent selective molecule, was found to be binding with MetAP2 in an irreversible way in covalent bonding. By repressing the MetAP2 expression in the cell, it was found to be acting as an anti-angiogenic compound that led to reduce the proliferation of fibroblast-like synoviocytes that originated inside joints in the synovium (Bainbridge et al., 2007)(Bernier et al., 2004).

2.3 Obesity

Obesity is the accumulation of fat cell in the body due to exceeding the amount of food that is usually needed or a lack of exercise. Diseases like diabetes or a genetic miss function like Prader–Willi syndrome can cause obesity or hyperplasia. A mixture of genetics, environmental and other factors can contribute to obesity. Being over-weight can be associated with many diseases such as hypertension, diabetes, liver steatosis, and it increases the chances of having a heart attack. Modern lifestyle choices have exceeded the ratio of obesity during these years due to the human limitation of activity and reliant on technology. The unbalance between food consumption and burning calories can cause obesity after a certain period. Therefore, changes are advised to patients with obesity by considering increasing their daily activities and going on a diet to prevent any future health-problems. However, as simple as that might sound or seem, many people find it hard to commit to a healthy lifestyle. In some cases long-term weight control is not always achievable through diet and, therefore, the drug design pharmaceutical industry has started investing in this field to find alternative ways to treat obesity and improve health.

The 2,4-Dinitrophenol (DNP), also known as amphetamine, is one of the first known anti-obesity drug out in the industry. DNP is a thyroid hormone drug used to treat obesity in the last century shows acceptable result. Sibutramine and Rimonabant are drugs also used to treat obesity, however, they were recently discontinued due to their severe side effects. The current available prescription medications for obesity patients are Amfepramone, Topiramate, and Lorcaserin. The path that these medications take to treat obesity is either by escalating the energy spending or reducing energy consumption without severe side effect. DNP, thyroid is using the escalation of energy spending pathway to efficiently lose weight. The other drugs that work to reduce energy consumption have much less side effect that the first types like Lorcaserin, and Phentermine with Topiramate, which considered as an anti-obesity factor.

The formation of the new blood vessel or the angiogenesis is offered an alternative solution in obesity drug design. Beside its role in cancer cell growth and metastatic angiogenesis process, it is also involved directly in obesity through modification of adipose tissue role in the cell which accommodates in their vessel wall a precursor cell through adiposeness which turns into adipocytes. These cells have their own growth and transcription factors which initiate the production either by their own or by another type such as an endothelial cell. This process is controlled by the angiogenesis.

Although inhibition of MetAP2 was originally designed to prevent cancer cell from growing and limit their resources, it was found tempted an important and continued weight loss. The mechanism that involves MetAP2 action is yet not have been discovered. However, the drug beloranib, which in fact is MetAP2 inhibition, was found to be arousing energy spending, fat consumption, and lipid elimination from the body. The study suggested using MetAP2 as an anti-angiogenic agent to target capillary vessels from increasing and spreading, hence, preventing the enlargement of adipose tissue which works as a treatment for obesity. CKD-732 is compound led from TNP-470 it is more efficient from the original towards the inhabitation of the enzyme and as result the reduction of the tumor. In vivo the drug has been tested with mice by introducing them with dosages for seven days. The results were remarkable as far as it goes for the size of the adipocytes as it showed a noticeable reduction.(Joharapurkar, Dhanesha and Jain, 2014).

2.4 Angiogenesis

The Angiogenesis concept was initially discovered in 1787 by a British doctor called John Hunter. In 1939 Ide and his colleagues conducted the first experiment which was later developed by Algire and Chalkley in 1945 to demonstrate the emergence of new blood vessel through a process called angiogenesis. Using a microspore filter, the researcher broke apart the tumors from the host tissue to verify that the undefined mysterious material that boosts the initiation of a new blood vessel was actually liberated from the tumor (Folkman, 1970).

Angiogenesis is the formation of new blood vessels. This procedure involves the migration, growth, and differentiation of endothelial cells, which line the inside wall of blood vessels. The significant role of angiogenesis appears of its participation in many diseases such as carcinoma, hematological, dermatology, ophthalmology and recently it has a feature role in eliminating obesity. The creation of the new blood vessel is conducted by two different mechanisms; Vasculogenesis and Angiogenesis. The Vasculogenesis is processed by which new blood vessel are created from progenitor cell into endothelial cells. By contrast, the Angiogenesis process is elucidated by the growth of new capillaries arise from already existed blood vessel (Ucuzian et al., 2010).

As the tumor grows, it requires a source of sustenance to expand and spread. The tumor increases and spread by exceeding the expression of the Angiogenesis compound in a cell. Vascular Endothelial Growth Factor (VEGF) is a signal protein created inside the cell, when it binds to its specific family of receptors, the promotion of new blood vessel starts. VEGF can also be initiated by the tumor which increases the proliferation of blood vessel (Nishida et al., 2006).

2.5 Methionine (Met)

Methionine (Met) is an alpha (α) amino acid that is indispensable for the human being due to the incapability of the cell to produce it. It is crucial for the cell, both structure and metabolism. In most enzymes, Sphero Proteins are found deep in the inner surface of the hydrophobic core (Brosnan et al., 2007). Methionine contains an amino group (NH₂), along with a carboxyl group (COOH), and Hydrogen(H) which is essential in all amino acid. But the S-methyl (CH₃S) thioester side chain is what distinguishes the methionine from the rest of the amino acid. Because of this side chain, the methionine is classified as a non-polar amino acid.

Methionine is coded by the first codon (AUG) that work as the first amino acid in the NH₂terminal position of a nascent polypeptide, which reveal its great importance in the synthesis of proteins (Guedes et al., 2011). Its remarkable role takes advantage in human due to its direct involvement in many diseases besides that was mentioned earlier such as Allergy, Schizophrenia, and Parkinson. On the other hand, the stimulation of cancer spread and metastases occur when an enormous amount of it exists in the cell. Keeping methionine under the required limit can prevent cancer from spreading and growing (Cavuoto and Fenech, 2012).

Fumagillin and Ovalicin are natural products that function as antiangiogenic and bind in an irreversible way to the MetAP2 and modify covalently histidine residue in the binding pocket (Catalano et al., 2001). TNP-470 a semisynthetic analog derived from fumagillin, show a significant selectivity against the molecular target MetAP2, when its traded to the animals, sustaining the possibility of future antiangiogenic analog used to prevent the cancer growth and other related diseases (Sheppard et al., 2004).

2.6 Methionine aminopeptidase II

Two main categories of MetAPs identified type 1 and type 2. Both categories are structurally alike but share slight sequence homology (Lowther and Matthews, 2000). The first type was found in the Eubacteria while type 2 was found in the archaeobacterial (Chang, McGary and Chang, 1989). Eukaryotes, on the other hand, retain both isoforms of MetAP 1 and 2 (Arfin et al., 1995). Remarkably, other forms of this enzyme were found in the chloroplasts and mitochondria which are (MetAP1B, MetAP1C, and MetAP1D) in the *Arabidopsis thaliana* plant (Giglione et al., 2000). The general structure of the MetAP, and all its forms, has a preserve C-terminal catalytic domain and inside the domain there are five different preserved amino acids that interact with two-metal cofactors known as cobalts (2Co). These amino acids are Aspartic acid 97, Histidine 171, Glutamic acid 204 and 235 (Roderick and Matthews, 1993). The distinguishable difference between the two isoforms is MetAP2 has an extra 60 amino acid in this domain, also the MetAP2 has thinner binding site than MetAP1 (Tahirov et al., 1998). The Mechanism of action is not yet been identified due to the lack of technology that enables the scientists to observe the hydrogen atoms through x-ray crystallography to recognize the bridging ligand (Korendovych et al., 2005). The suggested mechanism that is shown in figure 2.1 signifies the crucial role of the Histidine 178 and 79 that is highly preserved in all of the enzyme isoforms. Due to the catalytic characteristic of MetAP, the H79 transfers a proton to the N-terminal amine (Sin et al., 1997).

The two suggested mechanism of action of MetAP2 where (A) Tetrahedral intermediate alleviated by Glu204 and metal center. And (B) Tetrahedral intermediate alleviated His178 and metal center (Lowther et al., 1999). As mentioned previously, this enzyme function beside of the removal on the newly synthesized protein methionine residue to be functional the associating role in the endothelial cell proliferation and metastases (Griffith et al., 1997). The study that connected the MetAP2 is uncountable where the natural product fumagillin and its derivatives bind to the MetAP2 resulting inhibition of the angiogenesis processes (Larrabee, Chyun and

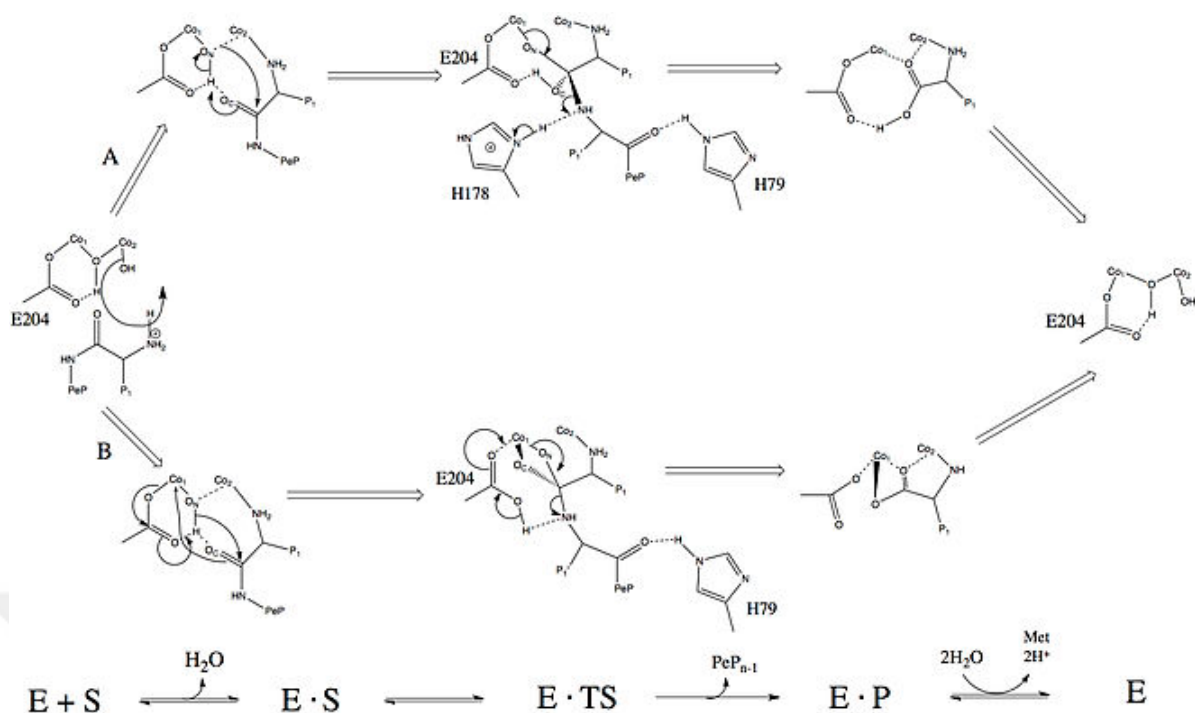


Figure 2.1 The two suggested mechanism of action of MetAP2 where (A) Tetrahedral intermediate alleviated by Glu204 and metal center and (B) Tetrahedral intermediate alleviated His178 and metal center (Lowther et al., 1999)

Volwiler, 2008), (Joharapurkar, Dhanesha, and Jain, 2014). The inhibitor of the MetAP2 beloranib has been presenting great potency as an anti-obesity drug candidate. Where the MetAP2 has the function for regulating the metabolism of the fat resulting in effective weight loss. Even with that, on the third phase of the clinical trial, the drug was discontinued (Kim et al., 2015).

2.7 Computer aid drug design

The great contribution that the computers provided in the field of the pharmaceutical industry reflected in the design and discovery of a new drug. The drug design branch provides a way of designing a drug without the need for huge funding. In the primary phases of developing the drug, computers provide an indispensable alternative in enhancing the drug bioactivity and selectivity feature that can be easily modified and improved through certain software and tools (Abdolmaleki, Ghasemi and Ghasemi, 2017).

2.7.1 Pharmacophore

Pharmacophore modeling approaches are an important part of computer-aided drug design that proves its significance through its various uses such as hit recognition, enhancing lead, and designing of novel drugs. The IUPAC describe the pharmacophore term as “an ensemble of steric and electronic features that is necessary to ensure the optimal supramolecular interactions with a specific biological target and to trigger (or block) its biological response” (Wermuth et al., 1998). It can be used to signify and illustrate molecules on schematic 2D or 3D level by categorizing the crucial possessions of molecular properties. Every kind of atom or group in a molecule can be condensed to a pharmacophore feature. These molecular arrangements would be categorized by some chemical properties, for example, hydrogen bond donors or acceptors, hydrophobic, etc., that can be later screened against databases and find a similar compound that shares these features (Yang, 2010). There are two approaches for pharmacophore modeling: Ligand-based and Structure-based pharmacophore modeling. The Ligand-based model is used when there is not enough information to obtain a protein structure. This approach emerges a solution strategy in the drug discovery process. The common chemical features are gathered from 3D ligands through alignment, which should signify the fundamental interaction between these inhibitors and the probable receptor that the research is aiming for (Vuorinen et al., 2014). The second approach, structure-based pharmacophore modeling, creates chemical features of the binding site and the satirical associations derived from the 3D structure of receptor or receptor-ligand complex. It investigates the likely of the interacting pattern between the receptor target and the ligands (Andricopulo, Salum and Abraham, 2009).

2.7.2 Virtual screening

The virtual screening is the process that is used in drug discovery to look for the compound that will most likely interact with the macromolecule target that can later serve as a drug candidate (Bohacek, McMartin and Guida, 1996). Using certain

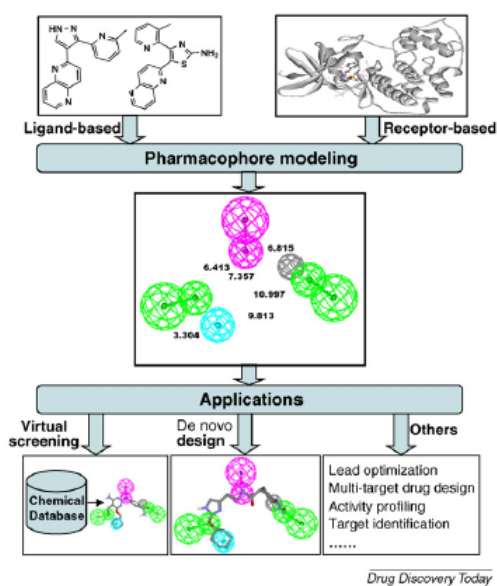


Figure 2.2 Pathway of the Pharmacophore Model (Andricopulo, Salum and Abraham, 2009)

software with virtual screening, this enables the researcher to look through very large databases with thousands or million compounds in couple of hours. Before the screening process takes place, the samples can be easily filtered to reduce the number of compounds in the data base using certain criteria such the Zinc15 and NCI. As the precision of the process is increasing along with uprising technology, it is becoming indispensable to the drug discovery field (McInnes, 2007).

2.7.3 ADMET Prediction Test

ADMET prediction is the procedure by which the computer anticipates the Absorption, Distribution, Metabolism, Excretion, and Toxicity of the compound. This procedure is fundamental in the drug discovery field because these features determine whether the compound can pass the clinical trials or not. Due to the huge funding that requires testing these characteristics in the lab, the researcher uses this approach. Usually, this approach used as filtration at the end of the drug discovery process (Cheng et al., 2013).

3. MATERIALS AND METHOD

This study was conducted using computer-aided drug design tools (in-silico) approach. The current study has shown two main methods that were performed to reach the results; Ligand-based pharmacophore model and second, Structure-based pharmacophore model (figure 3.1).

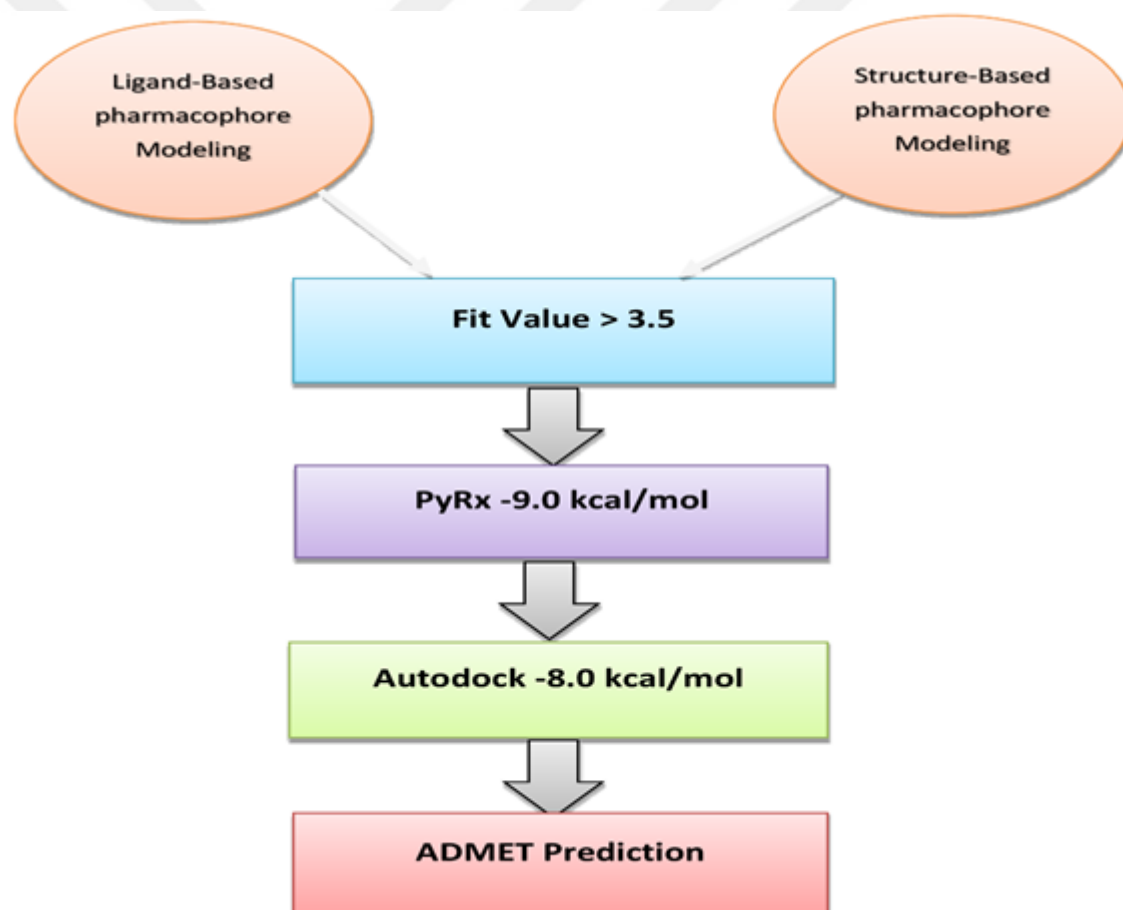


Figure 3.1 The procedure and the criteria that were followed while choosing the best inhibitor

The first approach uses a molecule that has known inhibition value of the enzyme, by constructing a common feature that is found in these inhibitors. The common chemical groups that construct the pharmacophore features are assumed to be fundamental. Whereas, the second approach, the receptor-ligand interaction type considers the foundation of building the pharmacophore feature. However, the chemical feature is either found between the receptor and its ligand or is not.



3.1 Database Preparation

The protocol “Build 3D Database” in Biovia Discovery Studio was used to construct a 3D database used in this study. The Zinc15 database was first chosen with over than two hundred and fifty million compounds commercially accessible to download (Sterling and Irwin, 2015). All compounds were pre-synthesized and prepared for virtual screening. The compounds are categorized according to different filters; moving horizontally from left to right across the Zinc15 platform shows an increasing in the molecular weight of the compound and moving vertically from upward to downward across the Zinc15 platform, the logP factor increases. The new advanced platform of Zinc15, Tranches, provided a beneficial feature of choosing according to Lipinski’s rule of five. To present an acceptable candidates for the drug-like molecules, the compounds were chosen based on specific standards; the scale of logP had to be from 1 to 5, the molecular weight from 250 to 500, number of Hydrogen-donors from 0 to 5, number of hydrogen acceptors from 0 to 9 and the rotatable bonds had to be less than 4 (Goodwin, Bunch and McGinnity, 2017). The number of compounds subject to these filtrations, was reduced to six million compounds.

A second database known as “The National Institute of cancer database (NCI) Release 4” was used to obtain needed data. The NCI database contains 266,151 SD file format with formulas, molecular weights, octanol/water partition coefficient KOW, and experimental logP (Milne et al., 1994). Lastly, the compound from both databases was uploaded to Biovia Discovery Studio using Build 3D database toolkit. The compound was used later for virtual screening in the research to obtain the best result according to Biovia DS fit value.

3.2 Ligand-Based Approach

3.2.1 Protein Preparation

The crystal structure of the enzyme Methionine aminopeptidase 2 (MetAP2) was chosen from the literature with a resolution of 1.75 ° A. According to the literature, it was obtained from human and it was mutation-free (Morgen et al., 2016). MetAP2 was downloaded from the “Protein Data Bank” database, under its PDB code 5CLS, and prepared using BIOVIA Discovery Studio 4.5 (Accelrys, Inc.). The protocol that performed the process was preceded by cleaning the protein from the native ligand, water molecule, and non-interacting ions. Proceeding with the process, the hydrogen atom was added to the protein and the Clean Geometry tool was used to optimize geometry using the force field. The final step includes ”preparing Macromolecule” protocol that cleans common issues that present in the protein structure and include the addition of the missing hydrogen based on the protonation state of the residues at PH of 7.4

3.2.2 Known Inhibitor, Molecular Docking Validation

The determination of the quality of the PDB structure that was chosen conducted by selecting known inhibitor of this enzyme. These inhibitors were obtained from the literature resembling the well-known inhibitor of this enzyme; some has Food and Drug Administration (FDA) approval and some still in different clinical trial phases. The Auto-dock automated docking tools (ADT) is a visualized tool and a generator of the docking files according to the ligand-receptor binding. It was employed to obtain the docking files that includes a grid parameter file (GPF) containing a map that stores all the potential energy of each atom in a ligand and a receptor that is used in the calculation in further steps. The second docking file is the docking parameter file (DPF) which has the receptor and the ligand names in PDBQT format, docking and search parameters (E^ˆsiyok et al., 2014). In Table 3.1 the ligands were docked into the binding site of the receptor to assure its accuracy.

The parameter was used for the (GPF) for each and every ligand 60, 60, 60 and the coordinates were 26.297, 21.191, and 16.855 were used as x, y, and z coordinate respectively.

Lastly, the Lamarckian Genetic algorithm was chosen and all the parameters were kept as a default except the number of energy evaluation, that was needed for the docking, it was set for twenty-five million, and the number of the GA runs was set to twenty to observe different conformations.

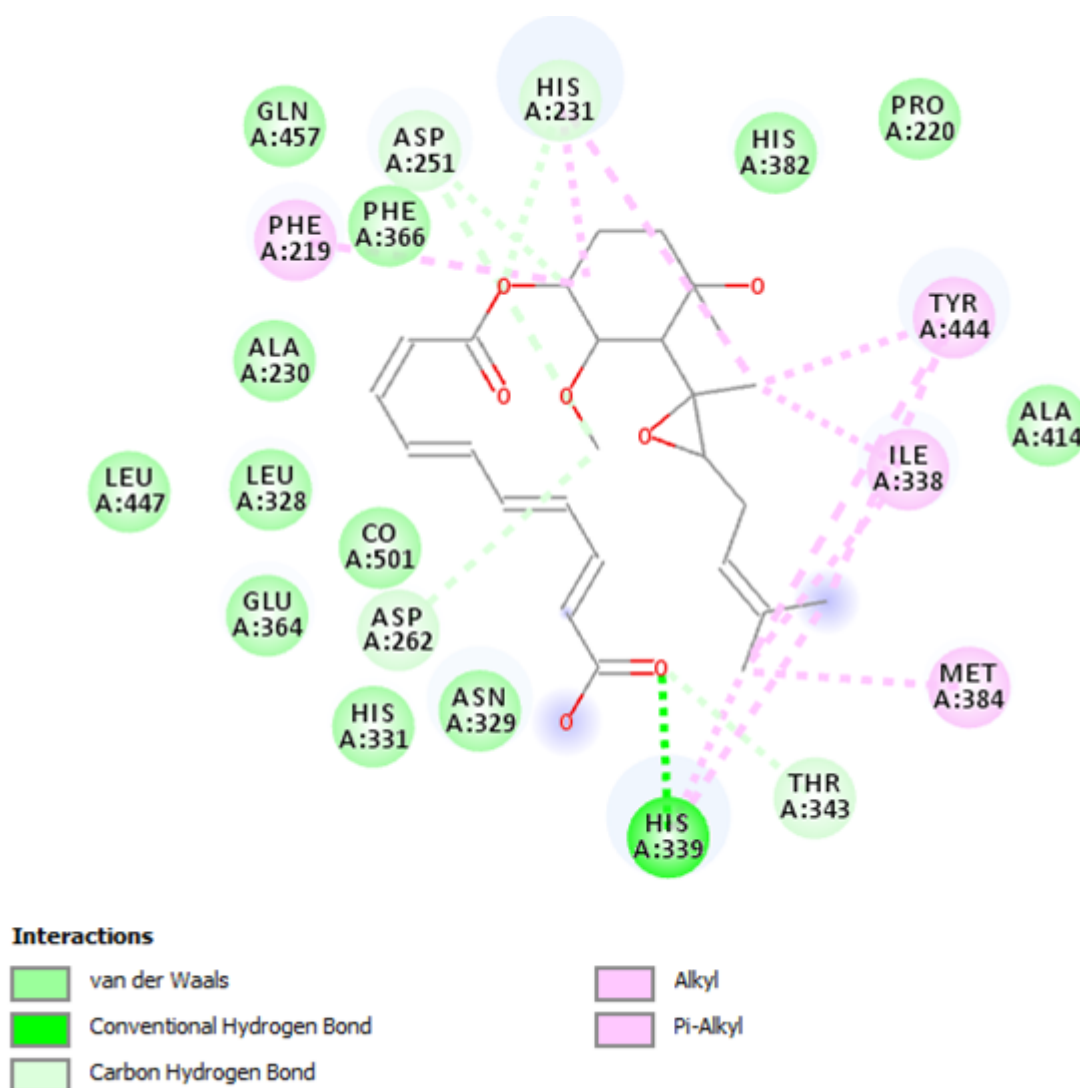


Figure 3.2 2D scheme showing diverse interactions such as Vander Waals, pi-sigma, Carbon Hydrogen bond, etc. between the receptor and Fumagillin

NO	Inhibitor	Binding Energy	Ki	IC50	Resource
1	5A	-9.14	198.36 nM	110.2 µM	(Çoruh <i>et al.</i> , 2018)
2	5B	-9.67	81.76 nM	16.0 µM	(Çoruh <i>et al.</i> , 2018)
3	5C	-9.37	135.51 nM	31.0 µM	(Çoruh <i>et al.</i> , 2018)
4	5D	-10.07	41.86 nM	7.22 µM	(Çoruh <i>et al.</i> , 2018)
5	5H	-9.80	66.09 nM	5.1 µM	(Çoruh <i>et al.</i> , 2018)
6	5K	-9.98	47.97 nM	6.48 µM	(Çoruh <i>et al.</i> , 2018)
7	5M	-9.73	73.31 nM	266.9 µM	(Çoruh <i>et al.</i> , 2018)
8	5N	-10.44	22.37 nM	19.77 µM	(Çoruh <i>et al.</i> , 2018)
9	5V	-11.74	2.48 nM	11.08 µM	(Çoruh <i>et al.</i> , 2018)
10	A-310840	-8.04	1.27 µM	61 nM	(Yin <i>et al.</i> , 2012)
11	A-357300	-9.80	65.62 nM	9 µM	(Yin <i>et al.</i> , 2012)
12	AGM-1470	-8.80	357.15 nM	50 pg/ml	(Kusaka <i>et al.</i> , 1991)
13	Compound 25	-9.45	118.66 nM	0.2 nM	(Arico-Muendel <i>et al.</i> , 2009), (Yin <i>et al.</i> , 2012)
14	Compound 29	-10.78	12.63 nM	0.048 µM	(Yin <i>et al.</i> , 2012)
15	Compound 30	-10.82	11.64 nM	0.19 µM	(Yin <i>et al.</i> , 2012)
16	Compound 31	-9.95	50.57 nM	0.13 µM	(Yin <i>et al.</i> , 2012)
17	Compound 50, A-800141	-8.76	380.07 nM	12 nM	(Yin <i>et al.</i> , 2012)
18	FUMAGILLIN	-9.05	232.47 nM	2 nM	(Kass <i>et al.</i> , 2012)
19	Iitraconazole	-8.97	266.05	0.16 µM	(Ehlers <i>et al.</i> , 2016)
20	JNJ4929821	-8.34	764.84 nM	15 nM	(Yin <i>et al.</i> , 2012)
21	PPI-2458	-8.64	465.29 nM	1.0.1nM 2. 0.2 nM	1.(Yin <i>et al.</i> , 2012) 2.(Bernier <i>et al.</i> , 2004)
22	Compound 8	-8.68	432.42 nM	1.15 µM	(Ehlers <i>et al.</i> , 2016)
23	CKD-732	-8.0	45.76 µM	0.65 nM	(Ehlers <i>et al.</i> , 2016)
24	Compound 6	-10.41	432.42 nM	1.2 µM	(Yin <i>et al.</i> , 2012)

Table 3.1 3.1 The known ligand used for validation of the macromolecule

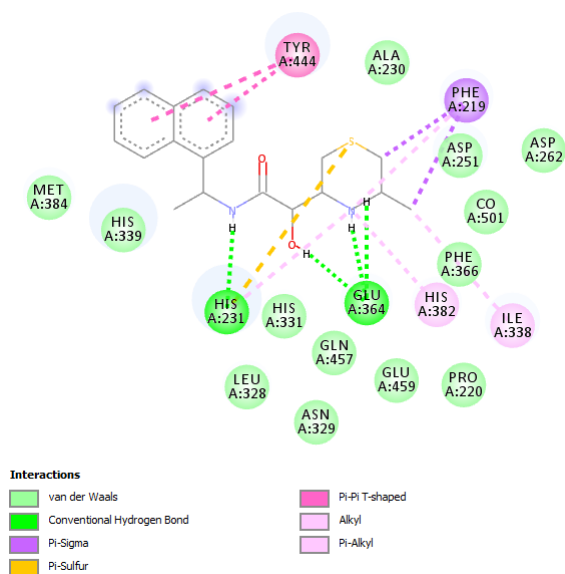


Figure 3.3 2D scheme showing diverse interactions such as Vander Waals, pi-sigma, pi-Sulfur, pi-Alkyl etc. Between the receptor and Compound 29

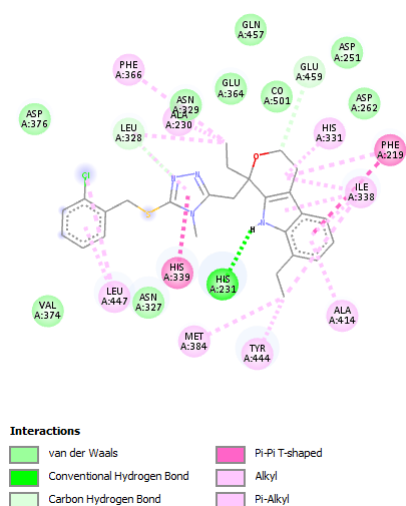


Figure 3.4 2D scheme showing diverse interactions such as Vander Waals, pi-sigma, Carbon Hydrogen bond, etc. Between the receptor and 5C

3.2.3 Data sets

The data set was obtained from a literature containing the known inhibitor for methionine aminopeptidase 2 (MetAP2). The main focus was to obtain a different compound that has diversity structure, an active compound which able to inhibit the MetAP2, and functioned as an anti-angiogenesis agent. In addition, the binding interaction of these well-known inhibitors with receptors, were taken into the account. All the inhibitors has IC50 and were synthesized and tested experimentally; some of them are in verity stages of the FDA clinical trial.



Inhipiter	IC50	Refrence
5A	110.2 μ M	(Çoruh <i>et al.</i> , 2018)
5B	16.0 μ M	(Çoruh <i>et al.</i> , 2018)
5C	31.0 μ M	(Çoruh <i>et al.</i> , 2018)
5D	7.22 μ M	(Çoruh <i>et al.</i> , 2018)
5H	5.1 μ M	(Çoruh <i>et al.</i> , 2018)
5K	6.48 μ M	(Çoruh <i>et al.</i> , 2018)
5M	266.9 μ M	(Çoruh <i>et al.</i> , 2018)
5N	19.77 μ M	(Çoruh <i>et al.</i> , 2018)
5V	11.08 μ M	(Çoruh <i>et al.</i> , 2018)
A-310840	61 nM	(Yin <i>et al.</i> , 2012)
AGM-1470	50 pg/ml	(Kusaka <i>et al.</i> , 1991)
Compound 8	1.15 μ M	(Ehlers <i>et al.</i> , 2016)
Iitraconazole	0.16 μ M	(Ehlers <i>et al.</i> , 2016)
Compound 6	1.2 μ M	(Yin <i>et al.</i> , 2012)
PPI-2458	1. 0.1nM 2. 0.2 nM	1.(Yin <i>et al.</i> , 2012) 2.(Bernier <i>et al.</i> , 2004)

Table 3.2 The Data set that was used to obtain the common pharmacophore feature

3.2.4 Pharmacophore Generation

The pharmacophore was generated using the "Common Features Pharmacophores Toolkit" in Biovia Discovery Studio 2016, where the conformation generation was set to best. The Maximum number of conformation generated was 255 along with energy threshold of 20 kcal/mol at the global minimum. The docked pose of the compound 5A obtained from the literature was used as a reference. The principal was set to 2 and MaxOmitFeat value was chosen as 0, and as for the remaining ligands, the first one was set to 1 and the second to 2 respectively (Wieder et al., 2016). Figure 3.5 shows the alignment of the compound that used.

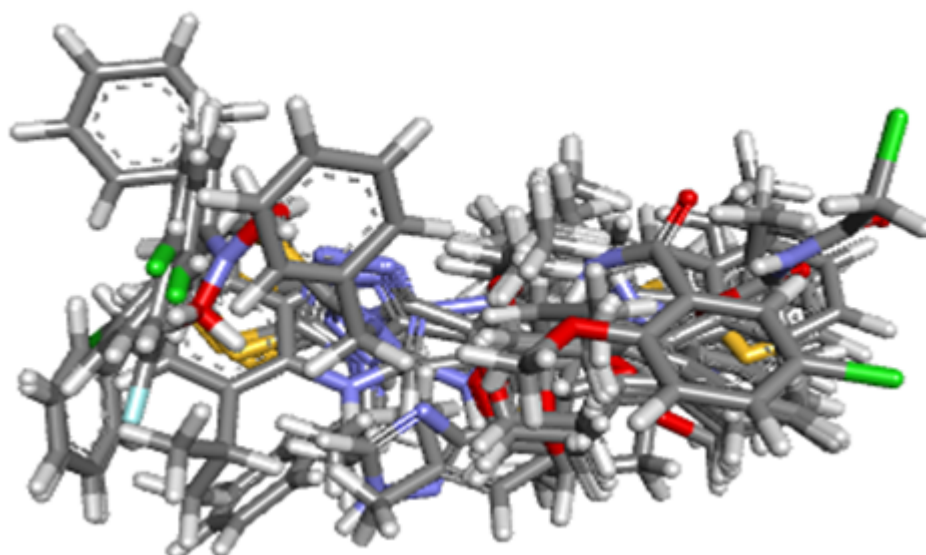


Figure 3.5 The compound that form the ligand based approach

After aligning the known inhibitors (Figure 3.5) that were obtained from the literature (Table 3.2), ten pharmacophore hypotheses (Figure 3.6) were generated using the protocol mentioned earlier. These hypotheses were assessed, along with the hypothesis from the Structure-Based approach, one by one using the Gunner-Henry method which will be mentioned later in this chapter.

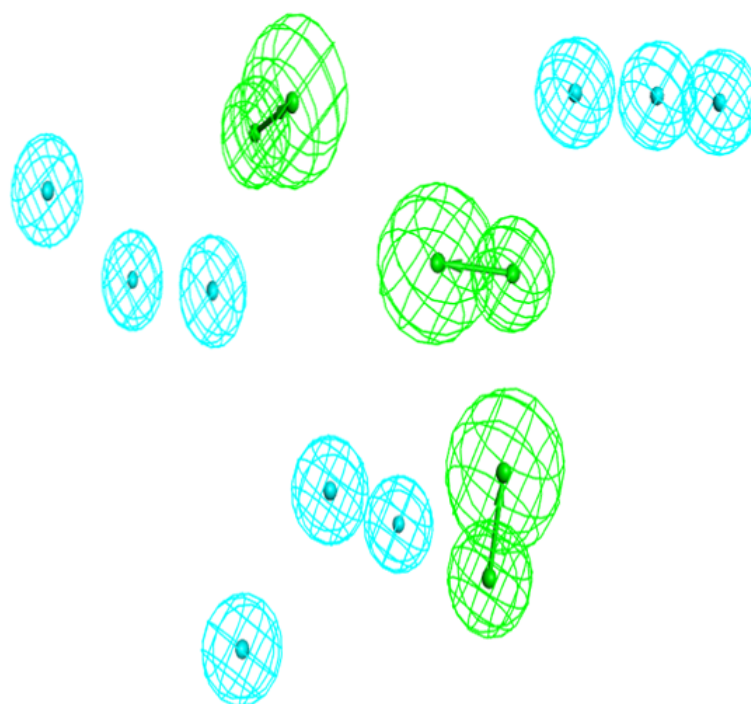


Figure 3.6 The Hypothesis that was generated using the data set obtained from the literature, the blue ball represented the hydrophobic feature while the green is the hydrogen bond acceptor

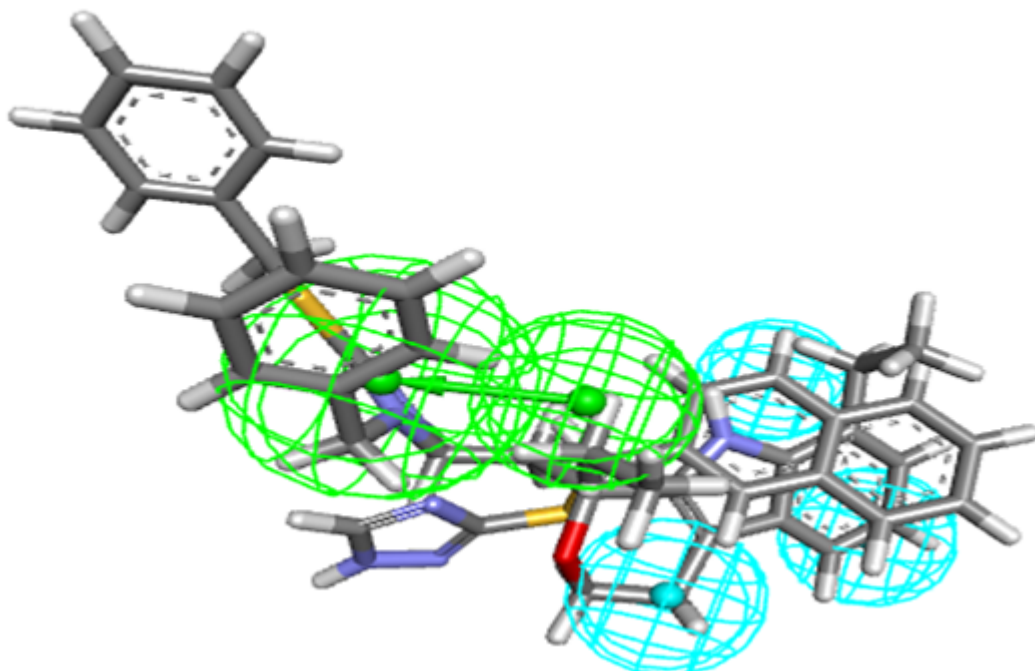


Figure 3.7 The two compounds 5n and A-310840 from the Data set aligning together and Mapping the pharmacophore hypothesis where the green represents hydrogen bond acceptor and the blue is the hydrophobic feature

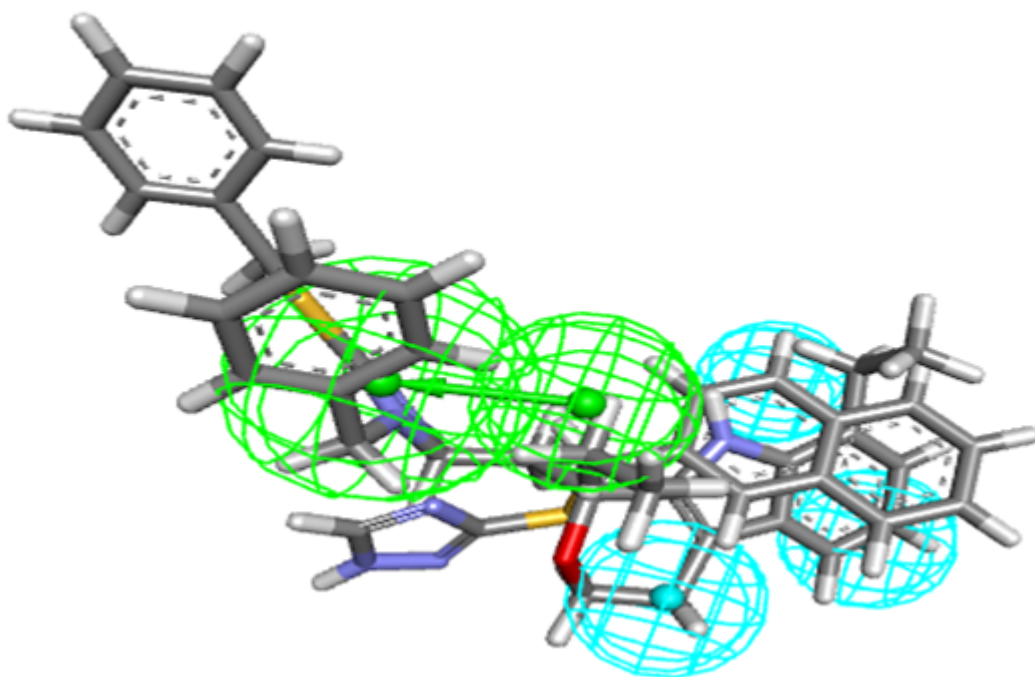


Figure 3.8 The Inhibitors Compound 8 and AGM-1470, from the Data, set aligning together and Mapping the pharmacophore hypothesis where the green represents hydrogen bond acceptor and the blue is the Hydrophobic feature

3.3 Structure-Based Approaches

This particular approach depends directly on the interaction between the receptor and the ligand in the 3D structure. The protocol was used to generate the hypotheses analysis of the chemical groups in the binding pocket and their locative relationships. The receptor-ligand-complex method used in this study was performed to identify the interacting groups between the ligands and the receptors.

The study proceeded by filtering the structure data so that only the proteins extracted from humans were chosen to be tested. The resolution of the X-ray was less than 2 Angstrom and there was no mutation in the structures that were obtained; they all shared the same Co-Factor which is Cobalt (Co). All the structures used in this section were obtained from the RCSB protein data bank under the PDB code 1B6A, 1B59, 1BOA, 1QZY, 2ADU, 2OAZ, 5D6E and 5D6F. (Liu et al., 1998), (Towbin et al., 2003), (Kallander et al., 2005), (Marino et al., 2007), (Morgen et al., 2016),

(Vuorinen and Schuster, 2015), (Yang, 2010).

3.3.1 Further Filtration

A further filtration was conducted using the phylogenetic tree protocol where Figure 3.9 was obtained. The reason behind using the phylogenetic tree is to take a closer look at the relationships between evolutionary related proteins where we can observe the evolutionary link between the proteins according to their sequence. Hence, a protein was chosen from each group that has similar sequences, where it's led to believe that they share a common ancestor.

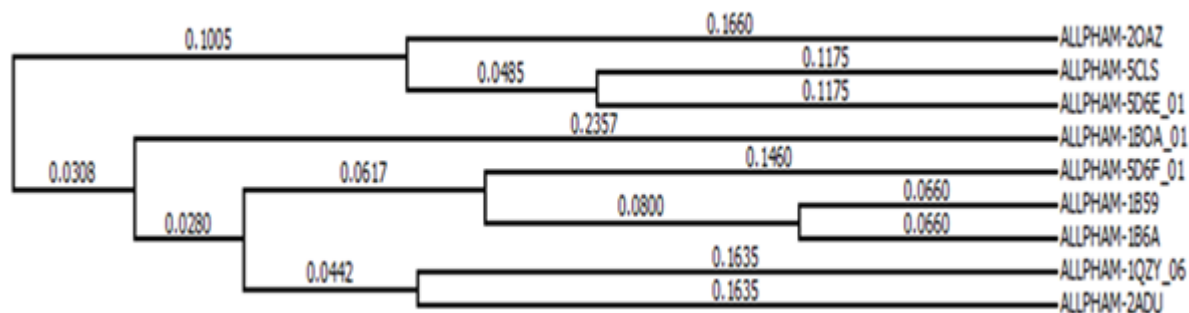


Figure 3.9 The phylogenetic tree of all input PDB structure

In Biovia Discovery Studio the phylogenetic tree protocol was used by including all the proteins as as input. According to the cluster, the elimination of the similar receptor-ligand structure, the pharmacophore model, was conducted to obtain only one of each group. The PDB 1BOA: MetAP2 is complexed with Fumagillin, 1QZY: MetAP2 with LAF153, and 5D6E, 5D6F: Metap2 with spiroepoxytriazole (-)-31and (+)-31br respectively. Those four complexes are the ones that have been chosen for the further steps in this study.

3.3.2 Protein Preparation

The proteins mentioned earlier were downloaded from the Protein data bank in PDB format. They were prepared for the next step by removing all water molecules from

each structure using the Biovia Discovery Studio 2016.

3.3.3 Pharmacophore Generation

The pharmacophore was generated using Biovia Discovery Studio where the pharmacophore generation receptor-ligand complexes protocol was used (Gaurav and Gautam, 2014). The generated hypothesis mimics the binding site between the receptor and the ligand, which will be used later for virtual screening to find similar but better ligands than the existing ones.

The 5D6E PDB complex resulted in 4 pharmacophore models with 6 features which was found between the receptor-ligand interacted point ,AAHHRR. In each of these models, there were the following features: hydrogen bond acceptor, hydrogen bond donor, hydrophobic and the aromatic ring. Both the selectivity score (6,6413) that was showed in the protocol report and the validation of the pharmacophore were taken into the consideration while choosing the best model between these four generated models. The figure 3.10 represent the pharmacophores that were selected for the screening.

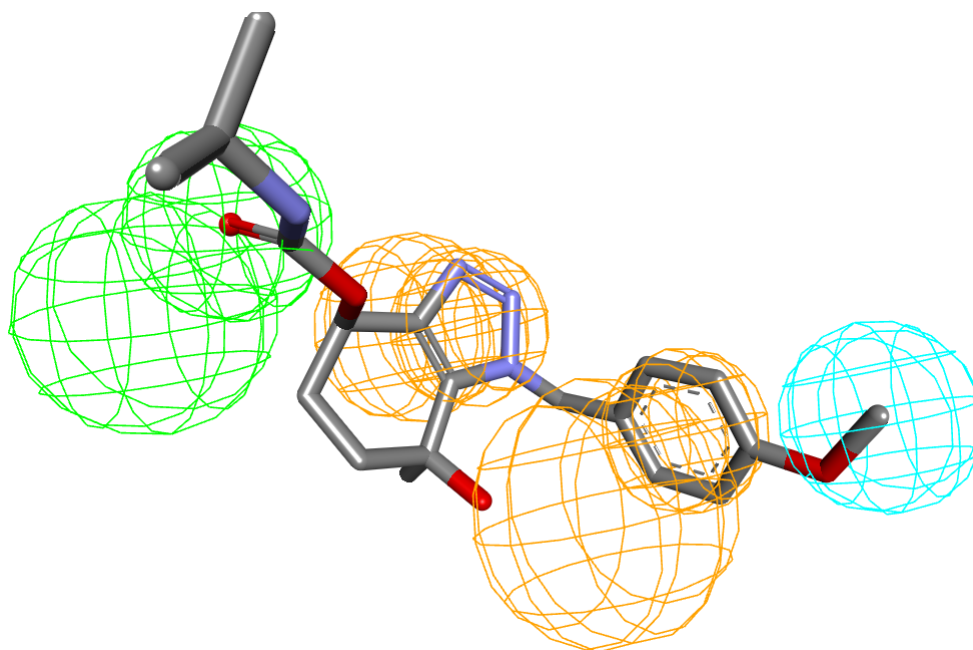


Figure 3.10 pharmacophore hypothesis of 5D6E complex

The 1BOA complex resulted in 10 models each with a different number of features and selectivity scores. The one that was selected (figure 3.11) has the highest number in both selectivity score 8,9325 and hydrophobic feature. According to a recent study, that assesses the pharmacophore feature consistency while using the molecular dynamic simulation, the hydrophobic feature is the most stabilized interaction out of the other features (Wieder et al., 2016). In figure 3.12 we can see the interaction between the ligand and the receptor that the generated model was based on.

In the figure 3.12 we can see the interaction between the ligand and the receptor that the generated model was based on.

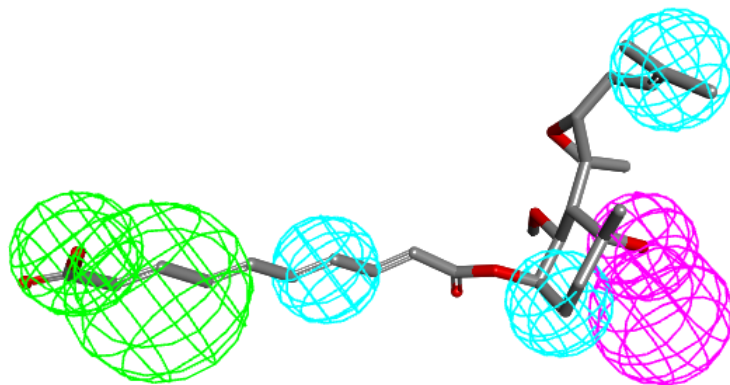


Figure 3.11 Best pharmacophore model of 1BOA complex

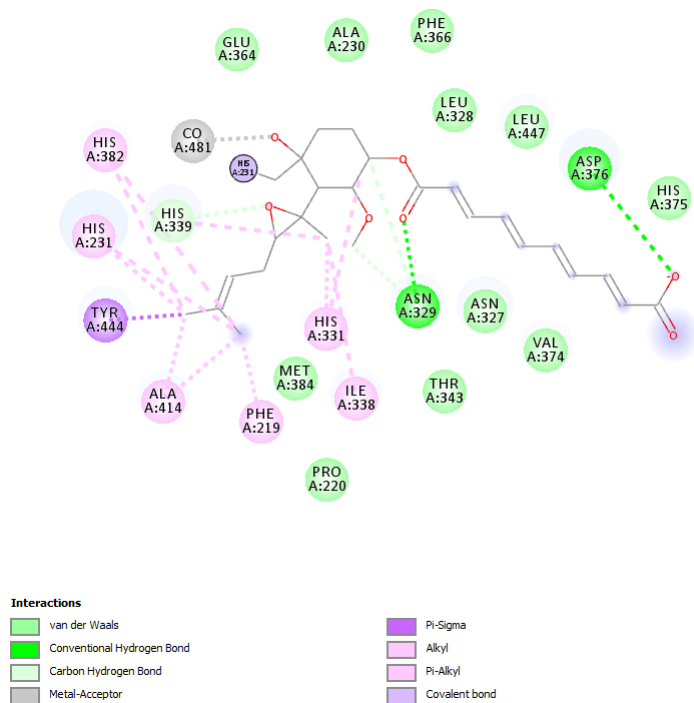


Figure 3.12 1BOA: MetAP2 in complex with Fumagillin

The 1QZY complex was resulted in the 10 pharmacophore models. The one that was selected, shown in figure 3.13, have six features; 4 Hydrogen acceptor, a Hydrogen donor, and Hydrophobic with selectivity score of 13,599.

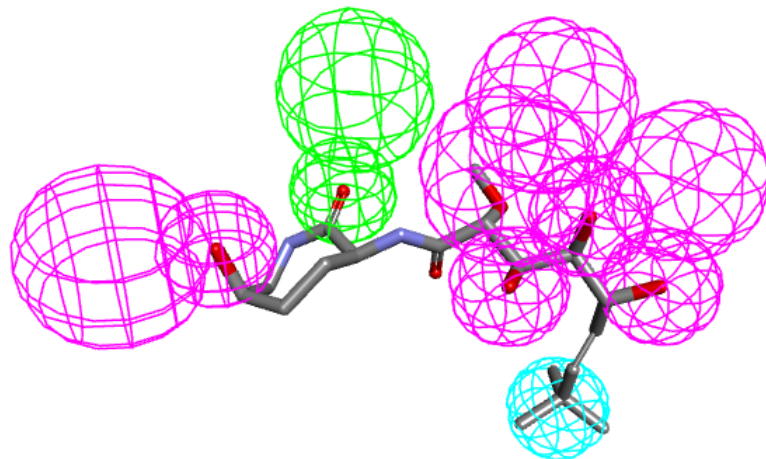


Figure 3.13 best pharmacophore model of 1QZY complex

The Figure 3.14 show the 2D interactions between the ligand and the receptor binding pocket.

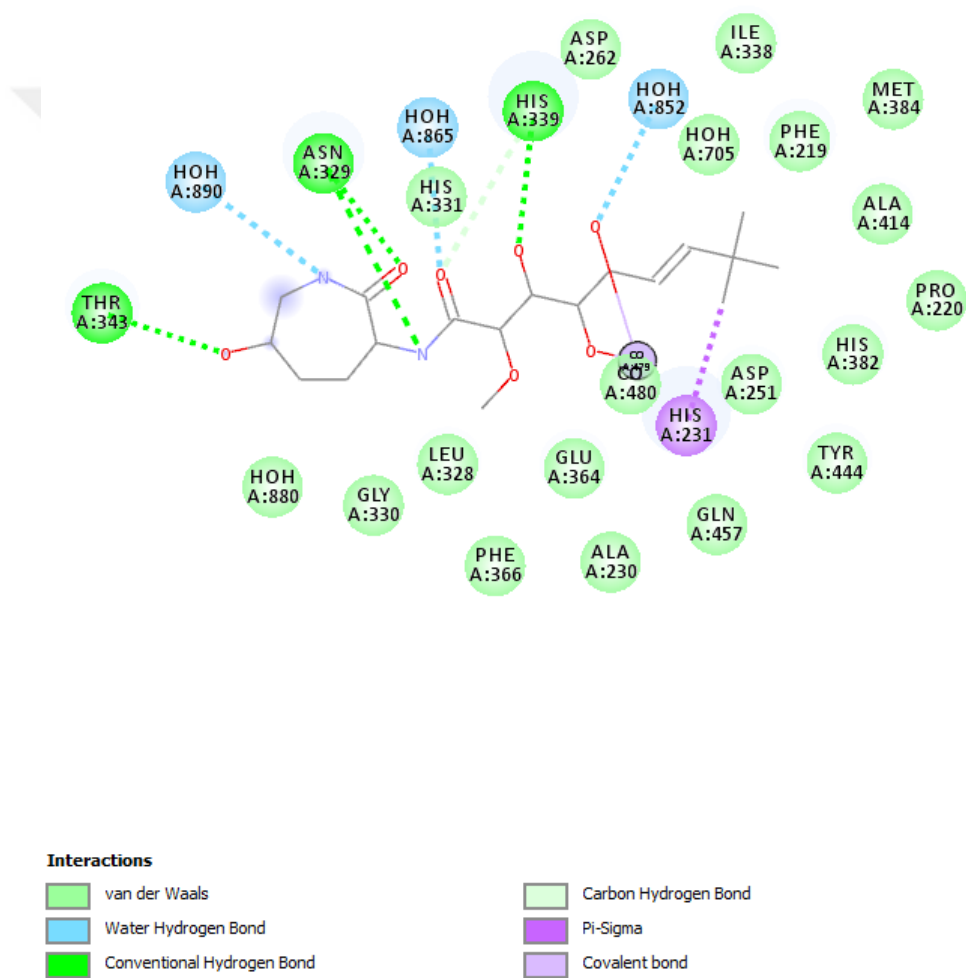


Figure 3.14 1QZY:MetAP2 in complex with LAF153 interacting in 2D

The 5D6F PDB complex generated 10 different models each with a different feature. The pharmacophore that was selected is shown in figure 3.15. It has the following features: two Hydrogen acceptors, Hydrophobic, Hydrogen donor, and an aromatic ring. The selectivity score of the assigned protocol was 11,429.

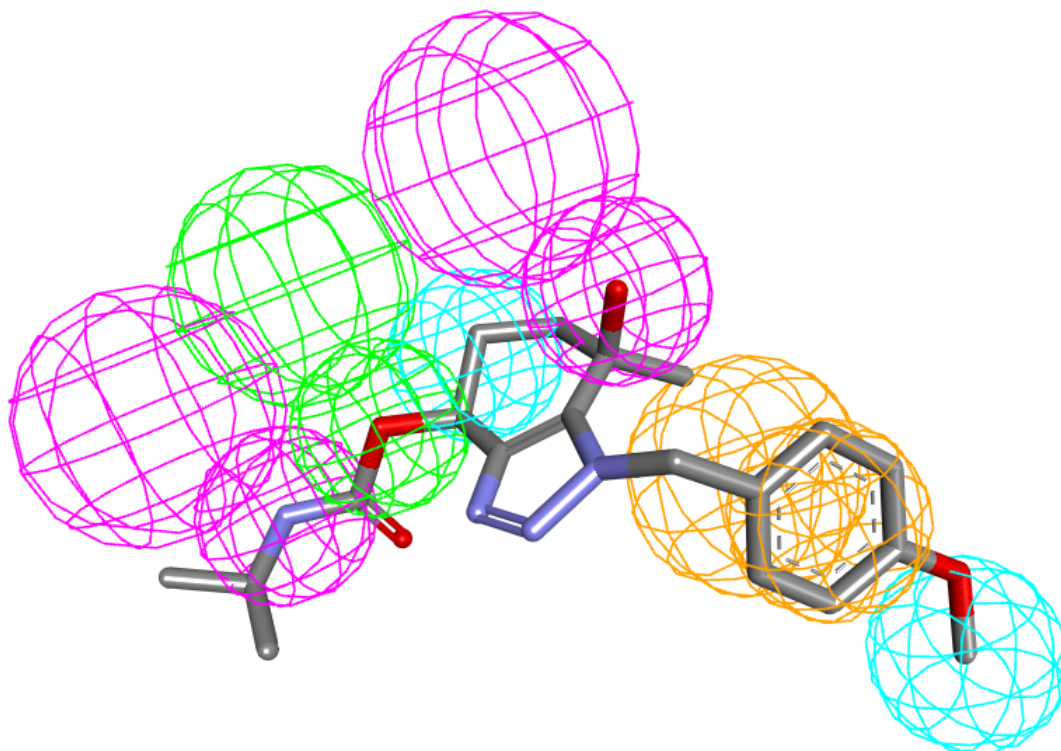


Figure 3.15 best pharmacophore model of 5D6F complex

Figure 3.16 show the 2D interaction between the ligand and the receptor in the complex that the feature was generated based on it.

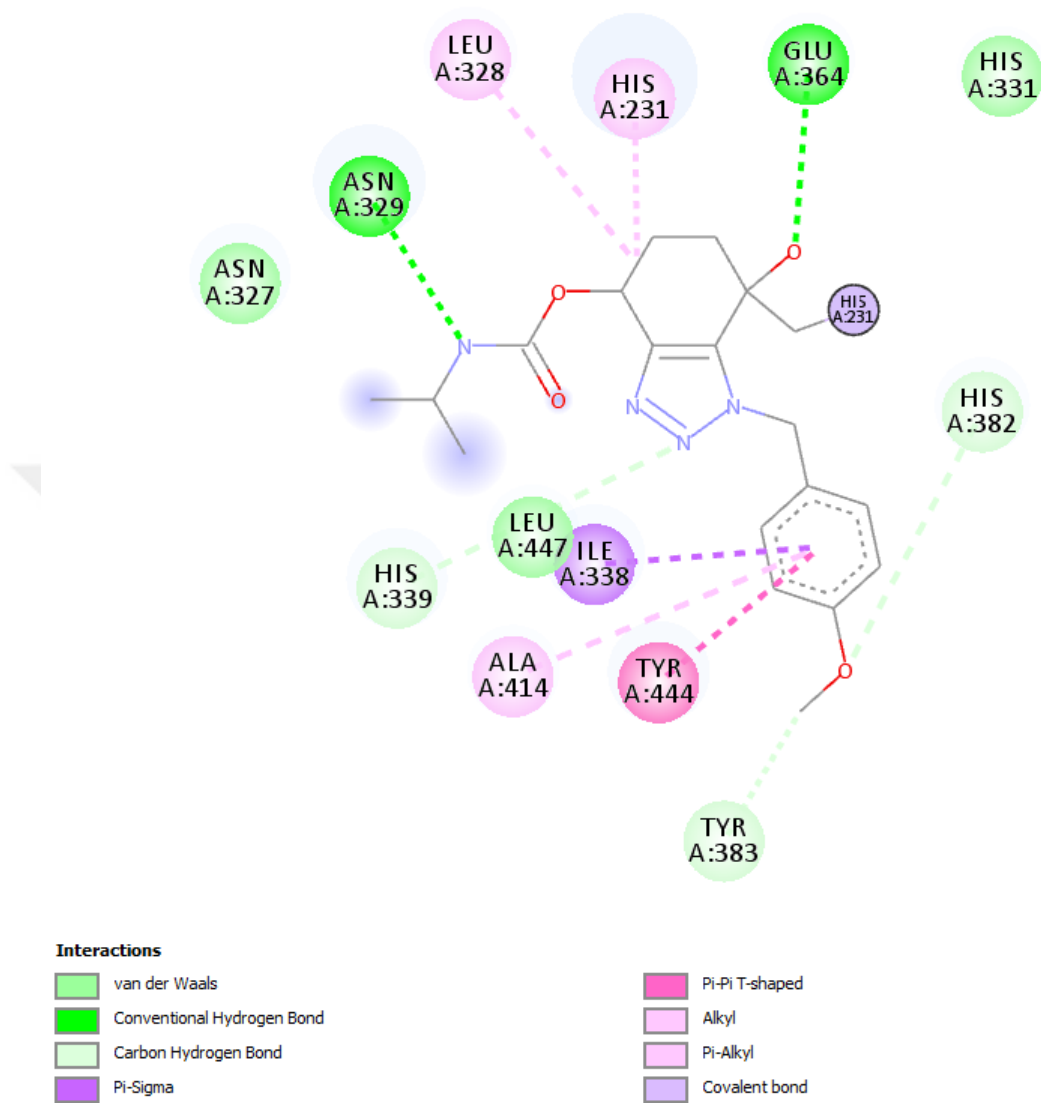


Figure 3.16 Best pharmacophore model of 5D6F complex

3.4 Pharmacophore validation

When it comes to the validation of the pharmacophore hypotheses that was generated using Biovia Discovery Studio 4.5, an active set was prepared to contain 39 active molecules obtained from literature and the native PDB ligand, which has IC50 (Table 3.3 and 3.4). The inactive set was prepared using a program called DecoyFinder-2.0; the set was taken from Zinc database which generates molecules that is inactive to the receptor that are used for pharmacophore generation (Adri'a, Garcia-Vallv'e, and Pujadas, 2012). The generated pharmacophore was evaluated using the equation provided by Gunner-Henry method:

$$\%A = \frac{Ha}{A} * 100$$

$$\%Y = \frac{Ha}{Ht} * 100$$

$$E = \frac{Ha/Ht}{A/D}$$

$$GH = \left(\frac{Ha(2A + Ht)}{4HtA} \right) \left(1 - \frac{Ht - Ha}{D - A} \right)$$

% A: The number of all the active compound in the database (accuracy).

Ha: The reiterative active hit (true positives).

A: The active molecule in the database.

% Y: The percentage of the active molecule extracted from the decoy set.

Ht: The number of hits in the database.

D: The number of the compound in the database.

E: The Enrichment Factor.

GH The Goodness of the Hit.

No	Inhibitor	IC50	Resource
1	5A	110.2 μ M	(Çoruh <i>et al.</i> , 2018)
2	5B	16.0 μ M	(Çoruh <i>et al.</i> , 2018)
3	5C	31.0 μ M	(Çoruh <i>et al.</i> , 2018)
4	5D	7.22 μ M	(Çoruh <i>et al.</i> , 2018)
5	5H	5.1 μ M	(Çoruh <i>et al.</i> , 2018)
6	5K	6.48 μ M	(Çoruh <i>et al.</i> , 2018)
7	5M	266.9 μ M	(Çoruh <i>et al.</i> , 2018)
8	5N	19.77 μ M	(Çoruh <i>et al.</i> , 2018)
9	5V	11.08 μ M	(Çoruh <i>et al.</i> , 2018)
10	A-310840	61 nM	(Yin <i>et al.</i> , 2012)
11	A-357300	9 μ M	(Yin <i>et al.</i> , 2012)
12	AGM-1470	50 nM	(Kusaka <i>et al.</i> , 1991)
13	Compound 25	0.2 nM	(Arico-Muendel <i>et al.</i> , 2009), (Yin <i>et al.</i> , 2012)
14	Compound 29	0.048 μ M	(Yin <i>et al.</i> , 2012)
15	Compound 30	0.19 μ M	(Yin <i>et al.</i> , 2012)
16	Compound 31	0.13 μ M	(Yin <i>et al.</i> , 2012)
17	Compound 50, A-800141	12 nM	(Yin <i>et al.</i> , 2012)
18	FUMAGILLIN	2 nM	(Kass <i>et al.</i> , 2012)
19	Iitraconazole	0.16 μ M	(Ehlers <i>et al.</i> , 2016)
20	JNJ4929821	15 nM	(Yin <i>et al.</i> , 2012)
21	PPI-2458	1.0.1nM 2.0.2 nM	1.(Yin <i>et al.</i> , 2012) 2.(Bernier <i>et al.</i> , 2004)
22	Compound 6	1.15 μ M	(Ehlers <i>et al.</i> , 2016)
23	CKD-732	0.65 nM	(Ehlers <i>et al.</i> , 2016)
24	Compound 8	1.2 μ M	(Yin <i>et al.</i> , 2012)
25	ovalicin	17.7 nM	(Yin <i>et al.</i> , 2012)
26	LAF153	1.6 nM	(Yin <i>et al.</i> , 2012)
27	A444148	1.4 μ M	(Sheppard <i>et al.</i> , 2006)
28	4-Aryl-1,2,3-triazole	18 nM	(Kallander <i>et al.</i> , 2005)
29	A773812	16 nM	(Wang <i>et al.</i> , 2007)
30	A193400	3 μ M	(Kawai <i>et al.</i> , 2006)

Table 3.3 The Training set that was used to validate the pharmacophore hypothesis-1

No	Inhibitor	IC50	Resource
31	SB-587094	Ki: 2 nM	(Marino <i>et al.</i> , 2007)
32	Spiroepoxytriazole	220 nM	(Morgen <i>et al.</i> , no date)
33	Fumarranol	3.2 uM	(Yin <i>et al.</i> , 2012)
34	Fumagalone	8 uM	(Yin <i>et al.</i> , 2012)
35	Bengamide B	0.0024um	(Yin <i>et al.</i> , 2012)
36	Bengamide E	3.3 nm	(Yin <i>et al.</i> , 2012)
37	Bengamide F	2.9-7.9 nM	(Yin <i>et al.</i> , 2012)
38	Bengamide P	1.2-7.9 nM	(Yin <i>et al.</i> , 2012)
39	Bengamide Z	1.5-2.9 nM	(Yin <i>et al.</i> , 2012)

Table 3.4 The Training set that was used to validate the pharmacophore hypothesis-2

Hypotheses	D	A	Ht	Ha	%A	%Y	E	GH
1	1881	39	31	30	76	96	46	0.917615711
2	1881	39	31	30	76	96	46	0.917615711
3	1881	39	31	29	74	93	45	0.886546701
4	1881	39	38	31	79	81	39	0.80747975
5	1881	39	39	31	79	79	38	0.791419583
6	1881	39	39	30	76	76	37	0.765472313
7	1881	39	38	31	79	81	39	0.80747975
8	1881	39	34	28	71	82	39	0.79453771
9	1881	39	38	31	79	81	39	0.80747975
10	1881	39	34	30	76	88	42	0.852217735
1BOA	1881	39	31	30	76	93	37	0.766666667
1QZY	1881	39	32	30	75	91	38	0.766666667
5D6E	1881	39	35	27	69	80	30	0.666304938
5DEF	1881	39	39	31	78	94	38	0.783333333

Table 3.5 The pharmacophore validation result for both Ligand-Based approaches, and Structure-Based approaches.

Table 3.5 shows the results of the implementation of the pharmacophore model that was generated earlier and later on processed in the equation of GunerHenry method to validate its accuracy (Guner, Clement and Kurogi, 2004). The GH scale is between 0 and 1, where the 1 represents the perfect score.

3.5 Virtual Screening

According to the previously validated results for both approaches, the selected models were searched via 3D query toolkit by Biovia Discovery Studio. The protocol that was preceded in this section called screening 3D databases. Both Zinc15 with over 6 million compounds and the National Institute of cancer NCI with over than 200 thousand compounds were screened. The Filtration was set to best and only the compounds with Fit Value higher than 3.5 were processed to the next step.

3.6 PyRx

PyRX is a free virtual scanning tool that uses the Autodock vina for screening number of drug potential targets. It is the user-friendly interfaces and the ability to add over 50 compounds in each run that makes it a very important tool in the drug discovery field (Zolfaghari, 2017). In order to filter the outcomes resulted from the screening, the compounds with a fit value over than 3.5 were selected. They were, then, extracted from the databases in form of PDB format file. For both approaches, the resulted compounds were docked in the macromolecules that were selected. In the ligand-based approach, the compounds with a fit value of 3.5 were all docked into the macromolecule 5CLS that was selected for the method. As for the structure-based approach, the compounds were docked to four macromolecules 1BOA, 1QZY, 5D6E and 5D6F. In a process called Cross-docking, all compounds were screened against the four macromolecules to ensure the output compounds are highly selective. During this process, the docking tool PyRx was used to obtain the high-affinity compounds. The criteria of the binding energy were set to 9.0 kcal/mol or higher by which the compounds were selected. The first two thousand compounds for each one of the hypotheses were proceeded through PyRx docking.

3.7 AutoDock

In the final docking process, the Autodock tools were used to obtain the binding energy and the K_i . The files were first generated using the grid parameter file (GPF) for each ligand and was set to 55, 55 and 55 in each dimension. The X, Y and Z Coordinates were set according to each macromolecule where the points in which the binding occur between macromolecule and ligand was extracted and used. The Lamarckian famous genetic algorithm was chosen while generating the docking parameter file (DPF). The GA run was set to 20 and the docking simulation run was set to 10,000,000 energy evaluations (Maruthanila et al., 2018).



4. RESULTS AND DISCUSSION

In this chapter, the results of the previous chapters will be demonstrated and discussed. The Ligand-Based pharmacophore Hypotheses and the Structure-Based pharmacophore Hypotheses were screened after validation. The databases Zin15 and the National Institute of Cancer (NCI) were screened using the Biovia Discovery Studio. After filtration using molecular modeling softwares, PyRx, and Autodock4, the results were obtained.

The final docking of the structure-based and the ligand-Based pharmacophore screening has yielded 20 compounds. The Ligand-Based approaches provided 10 compounds that have been docked to the 5CLS macromolecule and the Structure-Based approaches have 10 output compounds. That was cross-docked to each one of the three macromolecules 1BOA, 5D6E, and 5D6f to confirm the succeeded. To ensure the efficiency of these compounds criteria of 8.0 kcal/mol, threshold was implied. The compound for Ligand and Structure-Based methods are provided in Table 4.1 and 4.2, respectively. The cross-dock of the structure-based filter according to the binding energy was determined to be 8.0 Kcal/mol as shown in Table 4.3.

Code	Mwt	logP	ΔG Value Kcal/mole	Inhibition Constant(Ki) nM
ZINC000011791569	417	3.9	-9.79	66 nM
ZINC000011791570	445	4.4	-10.84	11 nM
ZINC000012191820	433	3.2	-9.94	51 nM
ZINC000012596578	371	4.1	-9.18	185 nM
ZINC12933720	385	2.3	-9.47	114 nM
ZINC000014019283	376	3.6	-10.02	45 nM
ZINC000012999580	394	2.3	-10.27	29 nM
ZINC000012222765	405	3.2	-12.10	1.35 nM
ZINC000011870844	474	2.2	-11.06	7.84 nM
ZINC000012953232	399	3.6	-10.66	15.39 nM

Table 4.1 Ligand-Based approaches the resulting compounds and their properties.

Code	Mwt	logP
ZINC48988425	425.872	2.9
ZINC000064968449	393.487	3.6
ZINC000014903160	383	3.9
ZINC000040174591	337	3.6
ZINC000095431249	312	2.6
ZINC000409110720	381	4.9
ZINC000066256921	332	2.9
ZINC000046087785	319	2.9
ZINC000015870630	391	4.1
ZINC15831093	324	2.5

Table 4.2 Structure-Based approaches the resulting compounds and their properties.

Code	1BOA ΔG Value Kcal/mole	1BOA Inhibition Constant (Ki)	5D6E ΔG Value Kcal/mole	5D6E Inhibition Constant (Ki)	5D6F ΔG Value Kcal/mole	5D6F Inhibition Constant (Ki)
ZINC48988425	-10.01	46 nM	-8.40	699nM	-10.88	10 nM
ZINC000064968449	-9.07	224nM	-9.21	177nM	-9.96	49 nM
ZINC000014903160	-9.24	168nM	-8.94	280nM	-9.31	149nM
ZINC000040174591	-9.75	71 nM	-9.65	84 nM	-9.35	140nM
ZINC000095431249	-8.49	593nM	-9.02	242nM	-8.88	309nM
ZINC000409110720	-9.22	174nM	-10.63	16 nM	-9.77	68 nM
ZINC000066256921	-8.19	1.0 uM	-8.46	626nM	-9.91	54 nM
ZINC000046087785	-8.23	926nM	-9.03	240nM	-8.37	727nM
ZINC000015870630	-9.60	92 nM	-10.65	15 nM	-10.22	32 nM
ZINC15831093	-8.50	587nM	-9.02	246nM	-8.56	527nM

Table 4.3 Structure-Based Cross-Docking between the different PDB Macromolecules.

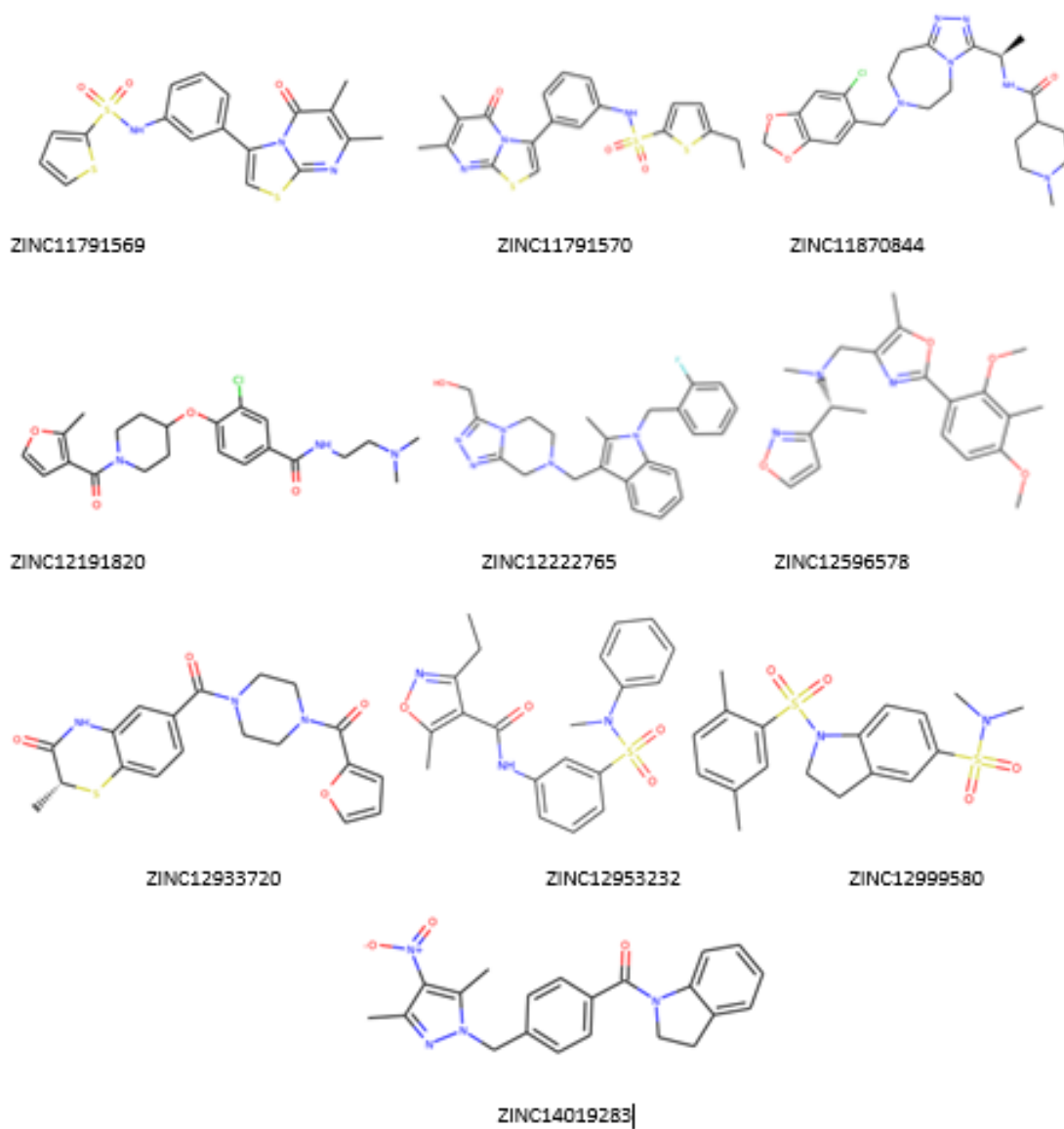


Figure 4.1 2D scheme Structure of the Inhibitor from the Ligand-Based approach's

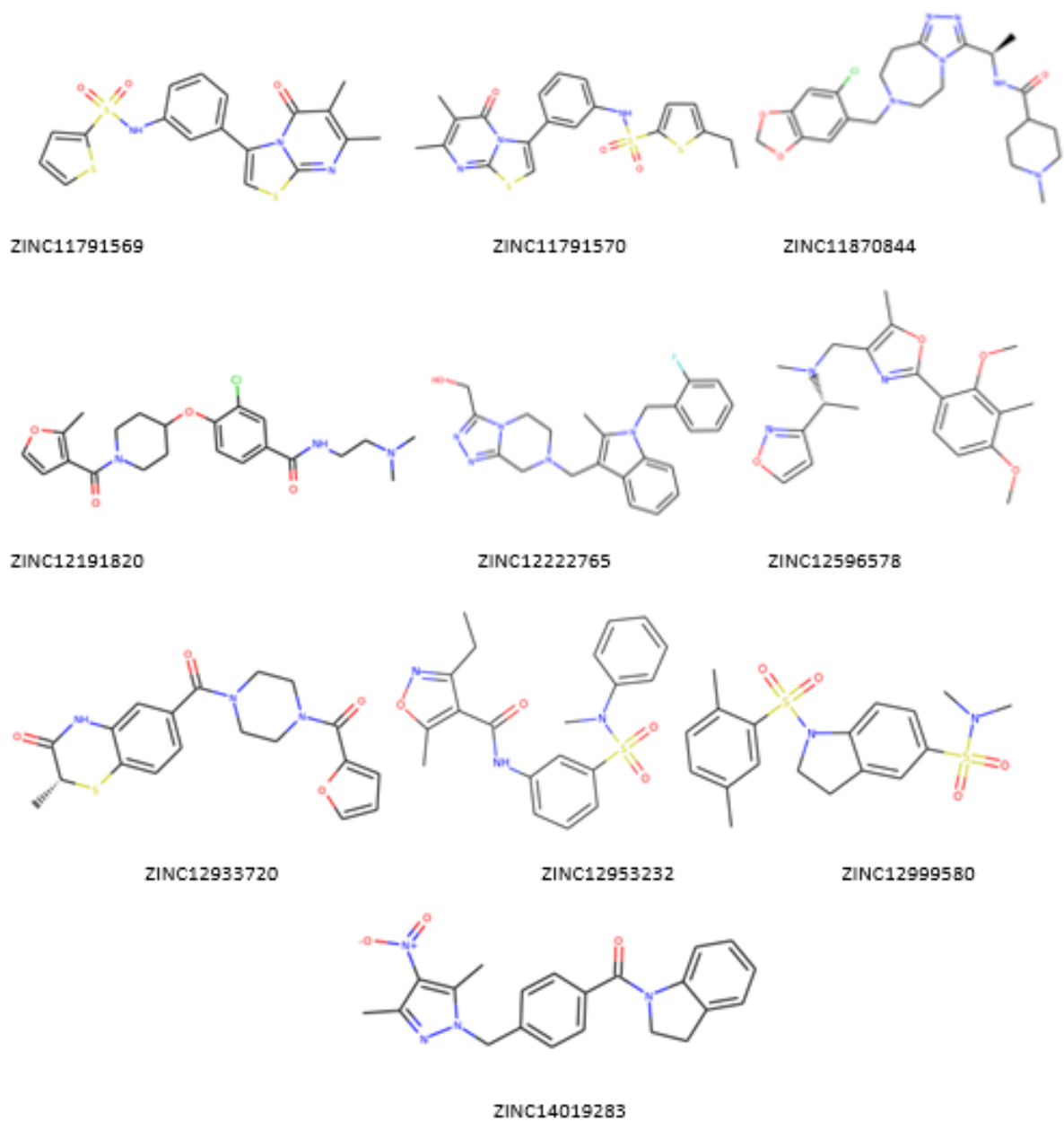


Figure 4.2 2D scheme Structure of the Inhibitor from the Structure-Based approach's

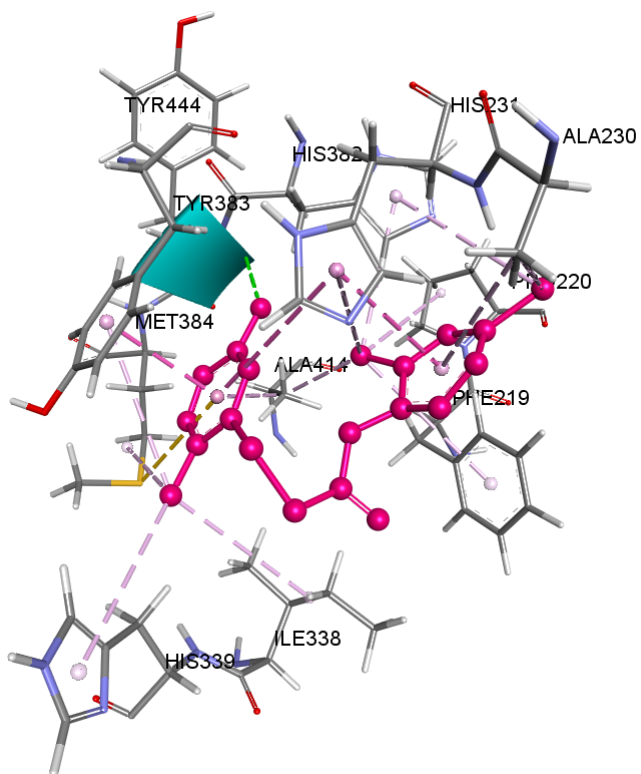


Figure 4.3 3D Interaction diagram between the amino acid residues and the binding pocket of 1BOA and ZINC000015831093

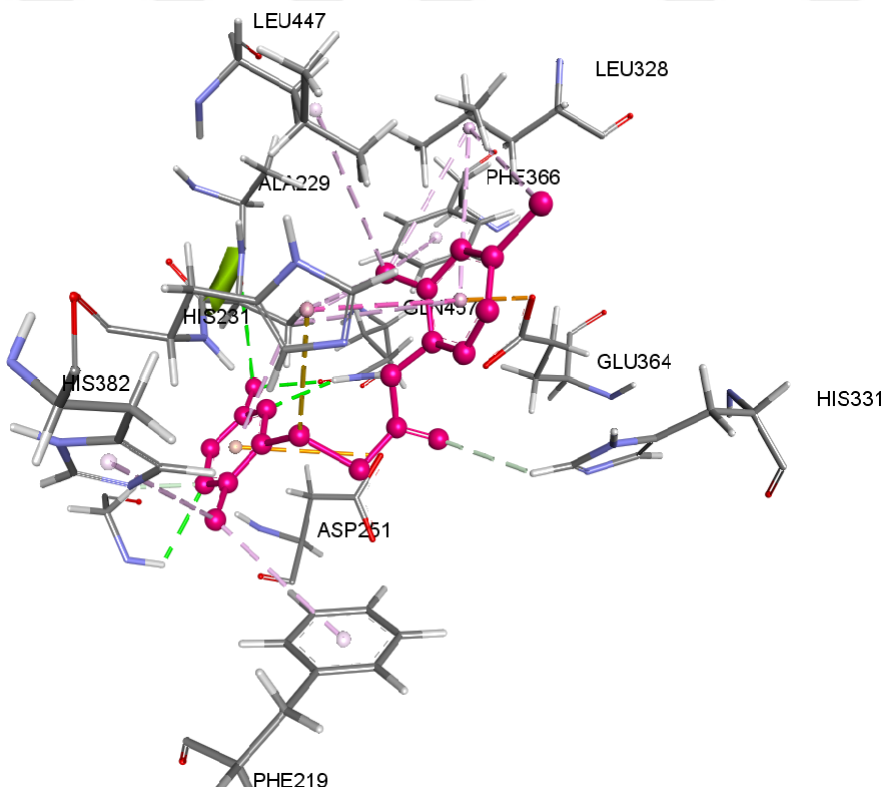


Figure 4.4 3D Interaction diagram between the amino acid residues and the binding pocket of 5D6E and ZINC000015831093

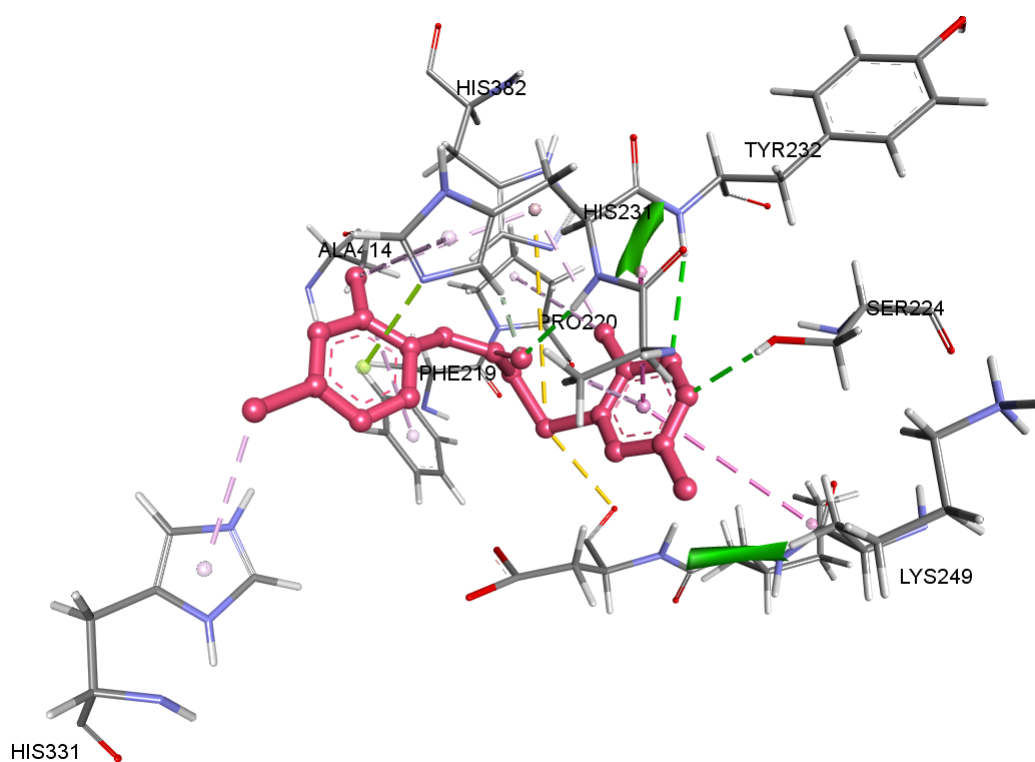


Figure 4.5 3D Interaction diagram between the amino acid residues and the binding pocket of 5D6F and ZINC000015831093

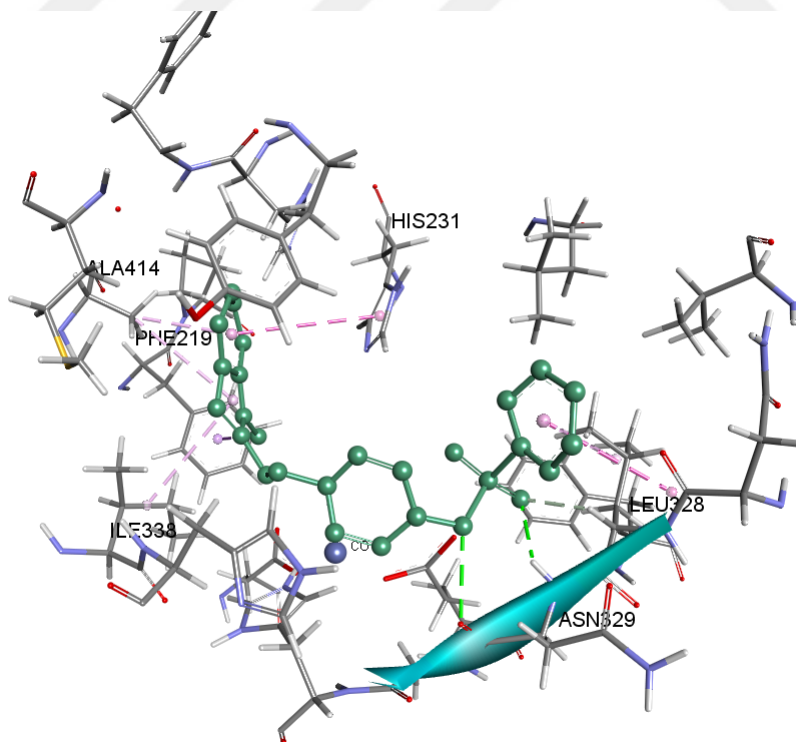


Figure 4.6 3D Interaction diagram between the amino acid residues and the binding pocket of 1BOA and ZINC000015870630

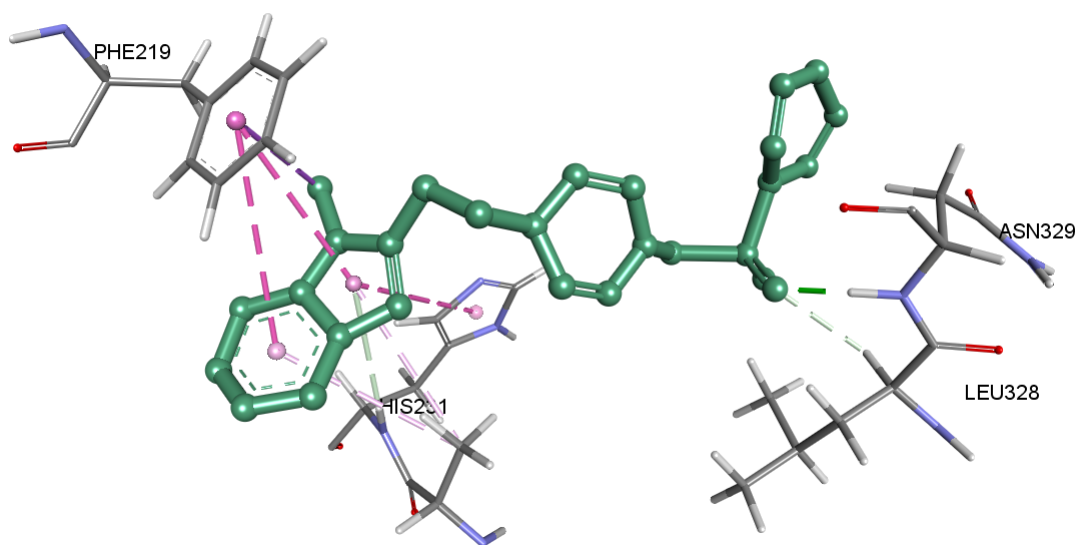


Figure 4.7 3D Interaction diagram between the amino acid residues and the binding pocket of 5D6E and ZINC000015870630

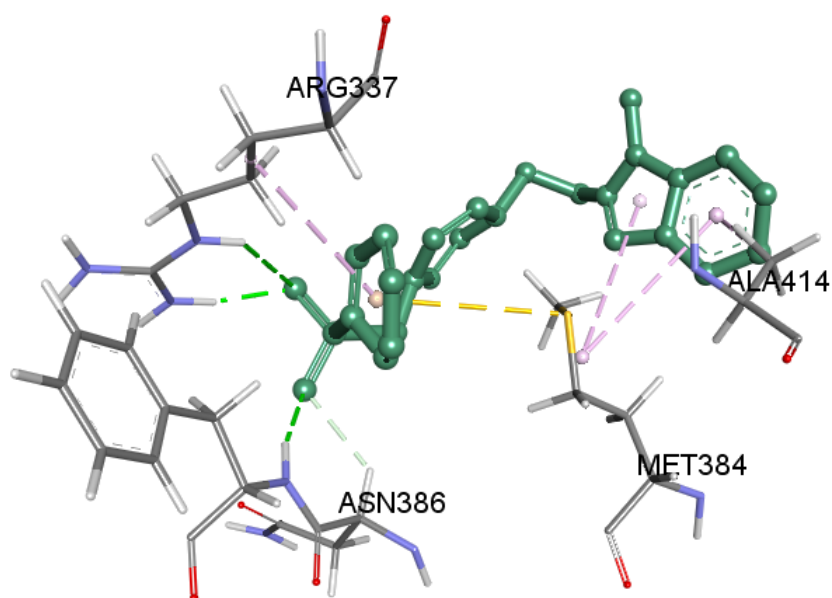


Figure 4.8 3D Interaction diagram between the amino acid residues and the binding pocket of 5D6F and ZINC000015870630

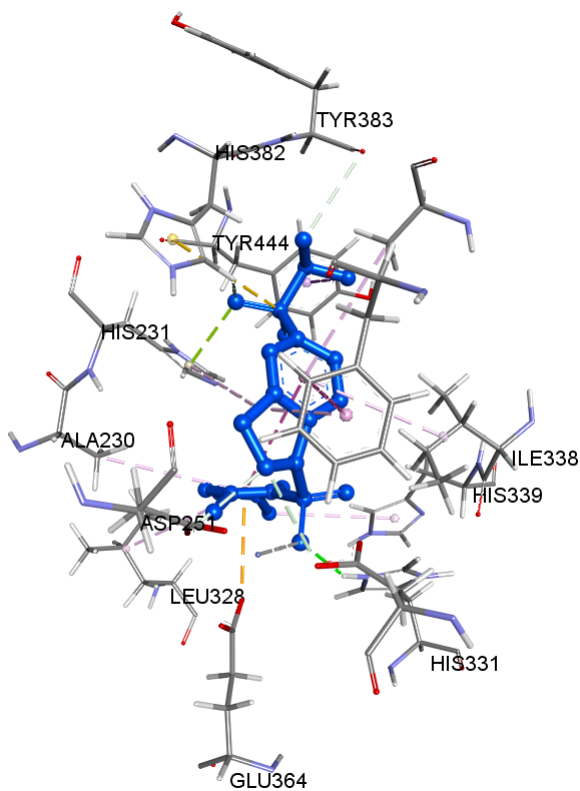


Figure 4.9 3D Interaction diagram between the amino acid residues and the binding pocket of 5cls and ZINC000012999580

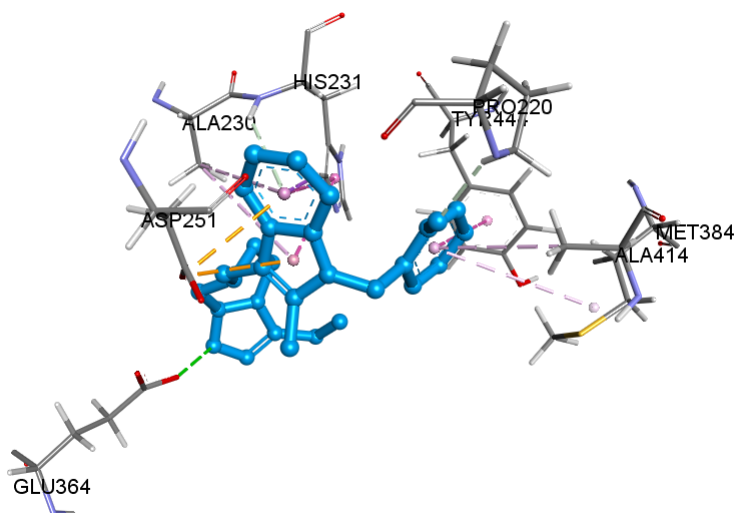


Figure 4.10 3D Interaction diagram between the amino acid residues and the binding pocket of 5cls and ZINC00001222765

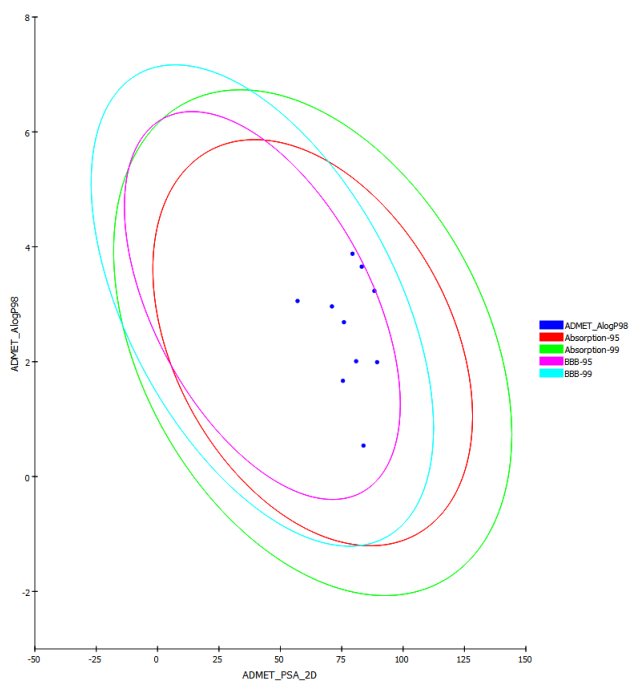


Figure 4.11 The calculated ADMET properties for the Ligand-Based inhibitors

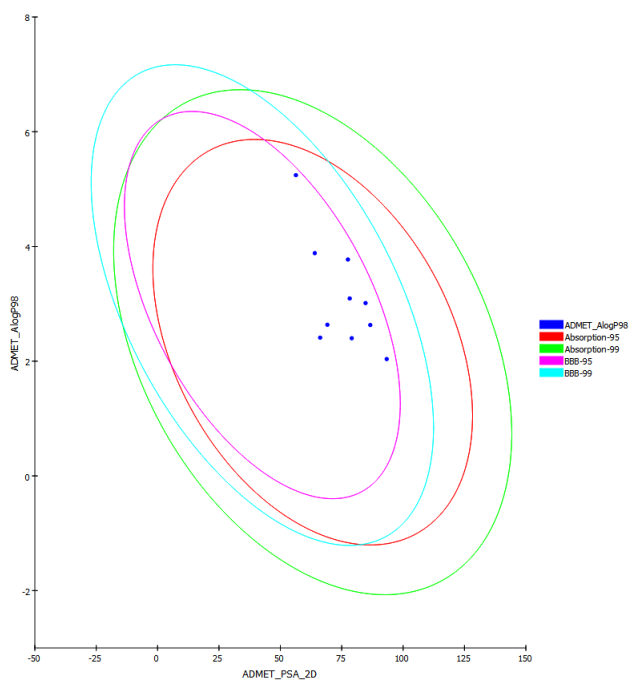


Figure 4.12 The calculated ADMET properties for the Structure-Based inhibitors

The study reveals twenty different compounds that have been selected through the previously described methodology. These compounds have been successfully passed all the barriers in the previous stage. First, through the virtual screening, the only compound with 3.5 fit values was processed. Next stage represents the screening using PyRx Virtual screening software the entire compound has to have 9.0 kcal/mol thresholds to be selected. Lastly, molecular docking was proceeded using Autodock4 tool with not less than 8.0 kcal/mol binding energy. The process to locate a good drug candidate is not enough without investigating its pharmacokinetics and pharmacology properties. Therefore, the next procedure was the ADMET production test that was conducted using Biovia Discovery Studio 2016. ADMIT prediction protocol contain Aqueous solubility, Blood-brain barrier penetration, Hepatotoxicity, Human intestinal absorption (HIA), Plasma protein binding. All of the chosen ones passed those criteria even though all the study was computational, choosing the databases that all compound are synthesized and available for the order will surely facilitate the biological test that can be made later to check these compound properties.

REFERENCES

- Abdolmaleki, A., Ghasemi, J. and Ghasemi, F. (2017) 'Computer Aided Drug Design for Multi-Target Drug Design: SAR /QSAR, Molecular Docking and Pharmacophore Methods', *Current Drug Targets*, 18(5), pp. 556–575. doi: 10.2174/1389450117666160101120822.
- Adrià, C. M., Garcia-Vallvé, S. and Pujadas, G. (2012) 'DecoyFinder, a tool for finding decoy molecules', *Journal of Cheminformatics* 2012 4:1. Nature Publishing Group, 4(1), p. P2. doi: 10.1186/1758-2946-4-s1-p2.
- Alberts, B. *et al.* (2002) 'Helper T cells and lymphocyte activation', in *Molecular Biology of the Cell*. doi: 10.1016/j.chembiol.2017.03.002.
- Anand, P. *et al.* (2008) 'Cancer is a preventable disease that requires major lifestyle changes', *Pharmaceutical Research*. doi: 10.1007/s11095-008-9661-9.
- Andricopulo, A., Salum, L. and Abraham, D. (2009) 'Structure-Based Drug Design Strategies in Medicinal Chemistry', *Current Topics in Medicinal Chemistry*. doi: 10.2174/156802609789207127.
- Arfin, S. M. *et al.* (1995) 'Eukaryotic methionyl aminopeptidases: two classes of cobalt-dependent enzymes.', *Proceedings of the National Academy of Sciences*. doi: 10.1073/pnas.92.17.7714.
- Arico-Muendel, C. C. *et al.* (2009) 'Carbamate analogues of fumagillin as potent, targeted inhibitors of methionine aminopeptidase-2', *Journal of Medicinal Chemistry*. doi: 10.1021/jm901260k.
- Bainbridge, J. *et al.* (2007) 'Methionine aminopeptidase-2 blockade reduces chronic collagen-induced arthritis: Potential role for angiogenesis inhibition', *Arthritis Research and Therapy*. doi: 10.1186/ar2340.
- Bernier, S. G. *et al.* (2004) 'A methionine aminopeptidase-2 inhibitor, PPI-2458, for the treatment of rheumatoid arthritis', *Proceedings of the National Academy of Sciences*. doi: 10.1073/pnas.0404105101.
- Bohacek, R. S., McMartin, C. and Guida, W. C. (1996) 'The art and practice of structure-based drug design: A molecular modeling perspective', *Medicinal Research Reviews*. doi: 10.1002/(SICI)1098-1128(199601)16:1;3::AID-MED1;3.0.CO;2-6.
- Brosnan, J. T. *et al.* (2007) 'Methionine: A metabolically unique amino acid', *Livestock Science*. doi: 10.1016/j.livsci.2007.07.005.
- Catalano, A. *et al.* (2001) 'Methionine aminopeptidase-2 regulates human mesothelioma cell survival: Role of Bcl-2 expression and telomerase activity',

American Journal of Pathology. American Society for Investigative Pathology, 159(2), pp. 721–731. doi: 10.1016/S0002-9440(10)61743-9.

Cavuoto, P. and Fenech, M. F. (2012) ‘A review of methionine dependency and the role of methionine restriction in cancer growth control and life-span extension’, *Cancer Treatment Reviews*. doi: 10.1016/j.ctrv.2012.01.004.

Chang, S. Y. P., McGary, E. C. and Chang, S. (1989) ‘Methionine aminopeptidase gene of *Escherichia coli* is essential for cell growth’, *Journal of Bacteriology*. doi: 10.1128/jb.171.7.4071-4072.1989.

Cheng, F. *et al.* (2013) ‘In Silico ADMET Prediction: Recent Advances, Current Challenges and Future Trends’, *Current Topics in Medicinal Chemistry*. doi: 10.2174/15680266113139990033.

Çoruh, I. *et al.* (2018) ‘Synthesis, anticancer activity, and molecular modeling of etodolac-thioether derivatives as potent methionine aminopeptidase (type II) inhibitors’, *Archiv der Pharmazie*. doi: 10.1002/ardp.201700195.

Ehlers, T. *et al.* (2016) ‘Methionine AminoPeptidase Type-2 Inhibitors Targeting Angiogenesis’, *Current Topics in Medicinal Chemistry*. doi: 10.2174/1568026615666150915121204.

Eşiyok, P. A. *et al.* (2014) ‘Aryl butenoic acid derivatives as a new class of histone deacetylase inhibitors: Synthesis, in vitro evaluation, and molecular docking studies’, *Turkish Journal of Chemistry*. doi: 10.3906/kim-1305-56.

Folkman, J. (1970) ‘History of Angiogenesis’, in *Angiogenesis [U+202F]: An Integrative Approach from Science to Medicine*. Springer, Boston, MA, pp. 1–2. doi: https://doi.org/10.1007/978-0-387-71518-6_1.

Gaurav, A. and Gautam, V. (2014) ‘Structure-based three-dimensional pharmacophores as an alternative to traditional methodologies’, *Journal of Receptor, Ligand and Channel Research*. doi: 10.2147/JRLCR.S46845.

Giglione, C. *et al.* (2000) ‘Identification of eukaryotic peptide deformylases reveals universality of N[U+2010]terminal protein processing mechanisms’, *The EMBO journal*. doi: 10.1093/emboj/19.21.5916 [doi].

Goodwin, R. J. A., Bunch, J. and McGinnity, D. F. (2017) ‘Mass Spectrometry Imaging in Oncology Drug Discovery’, in *Advances in Cancer Research*. doi: 10.1016/bs.acr.2016.11.005.

Griffith, E. C. *et al.* (1997) ‘Methionine aminopeptidase (type 2) is the common target for angiogenesis inhibitors AGM-1470 and ovalicin’, *Chemistry and Biology*. doi: 10.1016/S1074-5521(97)90198-8.

Guedes, R. L. M. *et al.* (2011) 'Amino acids biosynthesis and nitrogen assimilation pathways: A great genomic deletion during eukaryotes evolution', *BMC Genomics*. doi: 10.1186/1471-2164-12-S4-S2.

Guner, O., Clement, O. and Kurogi, Y. (2004) 'Pharmacophore Modeling and Three Dimensional Database Searching for Drug Design Using Catalyst: Recent Advances', *Current Medicinal Chemistry*. doi: 10.2174/0929867043364036.

Jayasekara, H. *et al.* (2016) 'Long-term alcohol consumption and breast, upper aero-digestive tract and colorectal cancer risk: A systematic review and meta-analysis', *Alcohol and Alcoholism*. doi: 10.1093/alcalc/agv110.

Joharapurkar, A. A., Dhanesha, N. A. and Jain, M. R. (2014) 'Inhibition of the methionine aminopeptidase 2 enzyme for the treatment of obesity', *Diabetes, Metabolic Syndrome and Obesity: Targets and Therapy*. doi: 10.2147/DMSO.S56924.

Kallander, L. S. *et al.* (2005) '4-Aryl-1,2,3-triazole: A novel template for a reversible methionine aminopeptidase 2 inhibitor, optimized to inhibit angiogenesis in vivo', *Journal of Medicinal Chemistry*. doi: 10.1021/jm050408c.

Kass, D. J. *et al.* (2012) 'Early treatment with fumagillin, an inhibitor of methionine aminopeptidase-2, prevents pulmonary hypertension in monocrotaline-injured rats', *PLoS ONE*. doi: 10.1371/journal.pone.0035388.

Kauczor, H. U. *et al.* (2015) 'ESR/ERS white paper on lung cancer screening', *European Radiology*. doi: 10.1007/s00330-015-3697-0.

Kawai, M. *et al.* (2006) 'Development of sulfonamide compounds as potent methionine aminopeptidase type II inhibitors with antiproliferative properties', *Bioorganic and Medicinal Chemistry Letters*. doi: 10.1016/j.bmcl.2006.03.085.

Kim, D. D. *et al.* (2015) 'Efficacy and safety of beloranib for weight loss in obese adults: A randomized controlled trial', *Diabetes, Obesity and Metabolism*. doi: 10.1111/dom.12457.

Korendovych, I. V. *et al.* (2005) 'Diiron(II) -aqua-hydroxo model for non-heme iron sites in proteins', *Inorganic Chemistry*. doi: 10.1021/ic051739i.

Kusaka, M. *et al.* (1991) 'Potent anti-angiogenic action of AGM-1470: comparison to the fumagillin parent', *Biochemical and Biophysical Research Communications*. doi: 10.1016/0006-291X(91)91529-L.

Kushi, L. H. *et al.* (2006) 'American Cancer Society Guidelines on Nutrition and Physical Activity for Cancer Prevention: Reducing the Risk of Cancer With

Healthy Food Choices and Physical Activity', *CA: A Cancer Journal for Clinicians*. doi: 10.3322/canjclin.56.5.254.

Larrabee, J. A., Chyun, S. A. and Volwiler, A. S. (2008) 'Magnetic circular dichroism study of a dicobalt(II) methionine aminopeptidase/fumagillin complex and dicobalt II-II and II-III model complexes', *Inorganic Chemistry*. doi: 10.1021/ic8011553.

Li, J. Y. *et al.* (2004) 'Mutations at the S1 sites of methionine aminopeptidases from *Escherichia coli* and *Homo sapiens* reveal the residues critical for substrate specificity', *Journal of Biological Chemistry*. doi: 10.1074/jbc.M401679200.

Liu, S. *et al.* (1998) 'Structure of human methionine aminopeptidase-2 complexed with fumagillin', *Science*. doi: 10.1126/science.282.5392.1324.

Lowther, W. T. *et al.* (1999) 'Insights into the mechanism of *Escherichia coli* methionine aminopeptidase from the structural analysis of reaction products and phosphorus-based transition-state analogues', *Biochemistry*. doi: 10.1021/bi991711g.

Lowther, W. T. and Matthews, B. W. (2000) 'Structure and function of the methionine aminopeptidases', *Biochimica et Biophysica Acta - Protein Structure and Molecular Enzymology*. doi: 10.1016/S0167-4838(99)00271-X.

Marino, J. P. *et al.* (2007) 'Highly potent inhibitors of methionine aminopeptidase-2 based on a 1,2,4-triazole pharmacophore', *Journal of Medicinal Chemistry*. doi: 10.1021/jm061182w.

Martin, T. A. *et al.* (2013) 'Cancer invasion and metastasis: Molecular and cellular perspective', in *Metastatic Cancer Clinical Biological Perspectives*. doi: 10.1607626.

Maruthanila, V. L. *et al.* (2018) 'In silico Molecular Modelling of Selected Natural Ligands and their Binding Features with Estrogen Receptor Alpha', *Current Computer-Aided Drug Design*, 15(1), pp. 89–96. doi: 10.2174/1573409914666181008165356.

McInnes, C. (2007) 'Virtual screening strategies in drug discovery', *Current Opinion in Chemical Biology*. doi: 10.1016/j.cbpa.2007.08.033.

Milne, G. W. A. *et al.* (1994) 'National Cancer Institute Drug Information System 3D Database', *Journal of Chemical Information and Computer Sciences*. doi: 10.1021/ci00021a032.

Morgen, M. *et al.* (2016) 'Spiroepoxytriazoles Are Fumagillin-like Irreversible Inhibitors of MetAP2 with Potent Cellular Activity.', *Acs Chem. Biol.*, 11, pp. 1001–1011. doi: 10.2210/PDB5CLS/PDB.

Morgen, M. *et al.* (2016) 'Spiroepoxytriazoles Are Fumagillin-like Irreversible Inhibitors of MetAP2 with Potent Cellular Activity', pp. 1–187.

Nishida, N. *et al.* (2006) 'Angiogenesis in cancer', *Vascular Health and Risk Management*. doi: 10.2147/vhrm.2006.2.3.213.

Roderick, S. L. and Matthews, B. W. (1993) 'Structure of the Cobalt-Dependent Methionine Aminopeptidase from *Escherichia coli*: A New Type of Proteolytic Enzyme', *Biochemistry*. doi: 10.1021/bi00066a009.

Sheppard, G. S. *et al.* (2006) 'Discovery and optimization of anthranilic acid sulfonamides as inhibitors of methionine aminopeptidase-2: A structural basis for the reduction of albumin binding', *Journal of Medicinal Chemistry*. doi: 10.1021/jm0601001.

Shimizu, H. *et al.* (2016) 'Methionine Aminopeptidase 2 as a Potential Therapeutic Target for Human Non-Small-Cell Lung Cancers', *Advances in Clinical and Experimental Medicine*, 25(1), pp. 117–128. doi: 10.17219/acem/60715.

Sin, N. *et al.* (1997) 'The anti-angiogenic agent fumagillin covalently binds and inhibits the methionine aminopeptidase, MetAP-2', *Proceedings of the National Academy of Sciences*. doi: 10.1073/pnas.94.12.6099.

Sterling, T. and Irwin, J. J. (2015) 'ZINC 15 - Ligand Discovery for Everyone', *Journal of Chemical Information and Modeling*. doi: 10.1021/acs.jcim.5b00559.

Tahirov, T. H. *et al.* (1998) 'Crystal structure of methionine aminopeptidase from hyperthermophile, *Pyrococcus furiosus*', *Journal of Molecular Biology*. doi: 10.1006/jmbi.1998.2146.

Towbin, H. *et al.* (2003) 'Proteomics-based target identification: Bengamides as a new class of methionine aminopeptidase inhibitors', *Journal of Biological Chemistry*. doi: 10.1074/jbc.M309039200.

Ucuzian, A. A. *et al.* (2010) 'Molecular mediators of angiogenesis', *Journal of Burn Care and Research*. doi: 10.1097/BCR.0b013e3181c7ed82.

Vuorinen, A. *et al.* (2014) 'Ligand-based pharmacophore modeling and virtual screening for the discovery of novel 17-hydroxysteroid dehydrogenase 2 inhibitors', *Journal of Medicinal Chemistry*. doi: 10.1021/jm5004914.

Vuorinen, A. and Schuster, D. (2015) 'Methods for generating and applying pharmacophore models as virtual screening filters and for bioactivity profiling', *Methods*. Elsevier Inc., 71(C), pp. 113–134. doi: 10.1016/j.ymeth.2014.10.013.

Wang, G. T. *et al.* (2007) 'Lead optimization of methionine aminopeptidase-2

(MetAP2) inhibitors containing sulfonamides of 5,6-disubstituted anthranilic acids', *Bioorganic and Medicinal Chemistry Letters*. doi: 10.1016/j.bmcl.2007.02.062.

Wermuth, C. G. *et al.* (1998) 'Chapter 36. Glossary of Terms Used in Medicinal Chemistry (IUPAC Recommendations 1997', *Annual Reports in Medicinal Chemistry*. doi: 10.1016/S0065-7743(08)61101-X.

Wieder, M. *et al.* (2016) 'Evaluating the stability of pharmacophore features using molecular dynamics simulations', *Biochemical and Biophysical Research Communications*. Elsevier Ltd, 470(3), pp. 685–689. doi: 10.1016/j.bbrc.2016.01.081.

Yang, S. Y. (2010) 'Pharmacophore modeling and applications in drug discovery: Challenges and recent advances', *Drug Discovery Today*. doi: 10.1016/j.drudis.2010.03.013.

Yin, S.-Q. *et al.* (2012) 'The Development of MetAP-2 Inhibitors in Cancer Treatment', *Current Medicinal Chemistry*. doi: 10.1007/s12275-010-9301-z.

Zolfaghari, N. (2017) 'Molecular docking analysis of nitisinone with homogentisate 1,2 dioxygenase', *Bioinformation*.